Sensitivity of photolysis frequencies and key tropospheric oxidants in a global model to cloud vertical distributions and optical properties

Hongyu Liu[1], James H. Crawford[2], David B. Considine[2], Steven Platnick[3], Peter M. Norris[3,4], Bryan N. Duncan[3,4], Robert B. Pierce[2,5], Gao Chen[2], and Robert M. Yantosca[6]

[1]National Institute of Aerospace, Hampton, VA

[2]NASA Langley Research Center, Hampton, VA

[3]NASA Goddard Space Flight Center, Greenbelt, MD

[4]University of Maryland, Baltimore County, MD

[5]Now at NOAA/NESDIS/STAR, WI

[6]Harvard University, Cambridge, MA

Short Title: Radiative Effects of Clouds: Sensitivity

Keywords: photolysis rate, tropospheric ozone, hydroxyl radical, solar radiation, cloud optical depth, cloud absorption, cloud overlap, 3-D global CTM

Manuscript submitted to Journal of Geophysical Research-Atmospheres; revised, Feb. 18, 2009

Correspondence: Hongyu Liu
Mail Stop 401B, NASA Langley Research Center
Hampton, VA 23681
Tel: 757-864-3191; Fax: 757-864-6326
Email: hyl@nianet.org

Abstract. Clouds affect tropospheric photochemistry through modification of solar radiation that determines photolysis frequencies. As a follow-up study to our recent assessment of the radiative effects of clouds on tropospheric chemistry, this paper presents an analysis of the sensitivity of such effects to cloud vertical distributions and optical properties (cloud optical depths (CODs) and cloud single scattering albedo), in a global 3-D chemical transport model (GEOS-Chem). GEOS-Chem was driven with a series of meteorological archives (GEOS1-STRAT, GEOS-3 and GEOS-4) generated by the NASA Goddard Earth Observing System data assimilation system. Clouds in GEOS1-STRAT and GEOS-3 have more similar vertical distributions (with substantially smaller CODs in GEOS1-STRAT) while those in GEOS-4 are optically much thinner in the tropical upper troposphere. We find that the radiative impact of clouds on global photolysis frequencies and hydroxyl radical (OH) is more sensitive to the vertical distribution of clouds than to the magnitude of column CODs. With random vertical overlap for clouds, the model calculated changes in global mean OH ($J(O^1D)$, $J(NO_2)$) due to the radiative effects of clouds in June are about 0.0% (0.4%, 0.9%), 0.8% (1.7%, 3.1%), and 7.3% (4.1%, 6.0%), for GEOS1-STRAT, GEOS-3 and GEOS-4, respectively; the geographic distributions of these quantities show much larger changes, with maximum decrease in OH concentrations of ~15-35% near the midlatitude surface. The much larger global impact of clouds in GEOS-4 reflects the fact that more solar radiation is able to penetrate through the optically thin upper-tropospheric clouds, increasing backscattering from low-level clouds. Model simulations with each of the three cloud distributions all show that the change in the global burden of ozone due to clouds is less than 5%. Model perturbation experiments with GEOS-3, where the magnitude of 3-D CODs are progressively varied from -100% to 100%, predict only modest changes (<5%) in global mean OH concentrations. $J(O^1D)$, $J(NO_2)$ and OH

concentrations show the strongest sensitivity for small CODs and become insensitive at large CODs due to saturation effects. Caution should be exercised not to use in photochemical models a value for cloud single scattering albedo lower than about 0.999 in order to be consistent with the current knowledge of cloud absorption at the ultraviolet wavelengths.

1. Introduction

Tropospheric ozone (O_3) is an important greenhouse gas, and hydroxyl radical (OH) determines the oxidative capacity of the troposphere [*Thompson*, 1992]. Any perturbations to O_3 and OH have important implications for climate change [*IPCC*, 2001]. Clouds affect tropospheric photochemistry through modification of solar radiation that determines photolysis frequencies [*Thompson et al.*, 1984; *Crawford et al.*, 1999], in addition to their roles in tropospheric chemistry via the processes of heterogeneous chemistry, wet removal, convective transport of trace gases and aerosols and nitrogen oxides (NO_x) emissions due to lightning associated with deep convective clouds. However, there have been few studies of the impact of clouds on photolysis frequencies and tropospheric oxidants such as O_3 and OH on a global scale [*Krol and van Weele*, 1997; *Tie et al.*, 2003; *Liu et al.*, 2006]. Cloud amounts and distributions may very well change in a changing climate and better understanding of the global impact of clouds is essential for predicting the feedback of climate change on tropospheric chemistry. We recently assessed the radiative effects of clouds on photolysis frequencies and key oxidants in the troposphere with GEOS-Chem [*Liu et al.*, 2006], a global three-dimensional (3-D) chemical transport model (CTM) driven by assimilated meteorological observations. In this paper, we apply the same model to examine the sensitivity of this effect to the uncertainty associated with the distributions and optical properties of clouds.

Modeling studies of the radiative effects of clouds on tropospheric chemistry have emphasized the need to account for the spatial and temporal variability of photolysis frequencies under different atmospheric (including cloud) conditions [*Wild et al.*, 2000; *Mao et al.*, 2003; *Tang et al.*, 2003; *Tie et al.*, 2003; *Yang and Levy*, 2004; *Liu et al.*, 2006]. Results indicated that photolysis frequencies are enhanced above and in the upper portion of cloud layers and are reduced below optically thick clouds, consistent with observations [*Lefer et al.*, 2003]. Including in the model the effect of vertical subgrid variability of cloudiness (cloud overlap) on radiative transfer has a significant impact on above-cloud (below-cloud) enhancements (reductions) [*Feng et al.*, 2004; *Liu et al.*, 2006]. Nevertheless, we found that regardless of the different assumptions about cloud overlap, the global average effect remained modest in GEOS-Chem when the model was driven by the GEOS-3 assimilated meteorology, reflecting an offsetting effect above and below clouds [*Liu et al.*, 2006]. This was consistent with the finding of *Krol and Weele* [1997] who found that the effect of clouds on the globally averaged lifetime of methane (CH_4) was small due to compensating effects above and below clouds.

Previous estimates of the radiative impact of clouds on global tropospheric chemistry were based on CTMs driven by different meteorology that contained different cloud fields, either from general circulation models (GCMs) [e.g., *Tie et al.*, 2003; *Wu et al.*, 2007] or from data assimilation systems [e.g., *Liu et al.*, 2006; *Wu et al.*, 2007]. The representation of clouds in current climate models is still a challenging task because cloud processes typically take place on scales that are not adequately resolved by these models and have to be parameterized [*Quante*, 2004; *Stephens*, 2005]. Recently, *Zhang et al.* [2005] compared clouds in ten GCMs and found that the majority of the models overestimated optically thick clouds by over a factor of 2, while underestimating optically intermediate and optically thin clouds. The uncertainty in simulated

clouds (and relevant radiative processes) has been recognized as a large limiting factor in current assessments of climate change [*IPCC*, 2001, 2007].

As a follow-up study to our recent assessment of the radiative effects of clouds on tropospheric chemistry [*Liu et al.*, 2006], this paper presents an analysis of the sensitivity of this effect to cloud vertical distributions and optical properties with the use of GEOS-Chem [*Bey et al.*, 2001; *Park et al.*, 2004] coupled with the Fast-J radiative transfer model [*Wild et al.*, 2000]. We drive GEOS-Chem with a series of meteorological archives from the Goddard Earth Observing System data assimilation system (GEOS DAS) at the NASA Global Modeling and Assimilation Office (GMAO), which are characterized by distinctly different cloud fields, in particular cloud vertical distributions and CODs. We will show that the radiative impact of clouds on global tropospheric chemistry is more sensitive to the vertical distribution of clouds than to the magnitude of CODs, and is also sensitive to the assumption about cloud absorption. We will also show that differing optical depths and vertical distributions of clouds cannot explain the contrasting sensitivities of tropospheric photochemistry to clouds in the two modeling studies of *Tie et al.* [2003] and *Liu et al.* [2006].

The paper is organized as follows. Section 2 gives a brief description of the GEOS-Chem model and its evaluation with observations. Section 3 presents the cloud fields in three GEOS meteorological archives and their evaluations with satellite observations. The sensitivities of photolysis frequencies and key oxidants to cloud vertical distributions, CODs, and cloud absorption of solar radiation are examined in sections 4 through 7, followed by summary and conclusions in section 8.

2. Model Description

GEOS-Chem is a global 3-D model of tropospheric O_3-NO_x-hydrocarbon chemistry coupled to aerosol chemistry, driven by assimilated meteorological observations with 3- to 6-hour resolution from the Goddard Earth Observing System (GEOS) of the NASA Global Modeling and Assimilation Office (GMAO). It solves the chemical evolution of ~90 species and transports 41 chemical tracers. The initial description of the model as applied to simulation of tropospheric O_3-NO_x-hydrocarbon chemistry was presented by *Bey et al.* [2001], with significant updates by *Martin et al.* [2002], *Park et al.* [2004] and *Evans and Jacob* [2005]. In particular, *Park et al.* [2004] coupled aerosol (including sulfate-nitrate-ammonium, carbonaceous aerosols, sea salt, and mineral dust) chemistry with O_3-NO_x-hydrocarbon chemistry. The model simulation of global tropospheric chemistry using different generations of GEOS assimilated meteorology has been evaluated in a number of studies since it was first evaluated by *Bey et al.* [2001]. The reader is referred to *Liu et al.* [2006] for a brief review. In this study we use GEOS-Chem version 7.1 (see http://www.as.harvard.edu/ctm/geos/) [*Heald et al.*, 2006; *Martin et al.*, 2006]. Global simulations of tropospheric chemistry were conducted for the years of 1996 and 2001. The simulation years were chosen so as to use different meteorological archives that have different cloud fields. All simulations in this study were conducted with five-month initialization and we analyze the model results for the years of 1996 and 2001.

Three generations of GEOS meteorological products are used for the simulation years as follows: GEOS1-STRAT for 1996 (2º latitude × 2.5º longitude horizontal resolution, 46 vertical levels, top at 0.1 hPa), GEOS-3 (1º latitude × 1º longitude, 48 levels, top at 0.01 hPa) and GEOS-4 both for 2001 (1º latitude × 1.25º longitude, 55 levels, top at 0.01 hPa, *Bloom et al.* [2005]). We have not included the latest GEOS-5 meteorological product because our main focus is on the sensitivity of tropospheric chemistry to different aspects (column integral and vertical

distribution) of the COD. The three archives used (GEOS1-STRAT, GEOS-3 and GEOS-4) provide continuity with our previous paper [*Liu et al.*, 2006] and provide enough variability in the COD distributions for the current sensitivity study. For computational expediency, we degrade the horizontal resolution to 4º×5º and merge the 23 (26, 36) vertical levels above 50 (85, 80) hPa for GEOS1-STRAT (GEOS-3, GEOS-4), retaining a total of 26 (30, 30) vertical levels. The vertical levels for GEOS1-STRAT and GEOS-3 are defined along a sigma coordinate. GEOS-4 employs a hybrid sigma-pressure coordinate system; the lowest 14 levels are pure sigma levels and the rest (mainly above 200hPa) fixed pressure levels. The midpoints of the lowest four levels in the GEOS1-STRAT (GEOS-4) data are at 50 (60), 250 (250), 600 (610), and 1100 (1200) m above the surface for a column based at sea level. The GEOS-3 data have finer resolution of the boundary layer with layer midpoints at 10, 50, 100, 200, 350, 600, 850, and 1250m above the surface. The cross-tropopause flux of O_3 is specified with the Synoz (synthetic O_3) scheme [*McLinden et al.*, 2000] by imposing a global net cross-tropopause flux of 475 Tg O_3 per year (GEOS1-STRAT), 500 Tg O_3 per year (GEOS-3), and 495 Tg O_3 per year (GEOS-4); the variability partly reflects the difference in circulations between meteorological archives. A uniform global CH_4 concentration of 1700 ppbv is imposed.

Photolysis frequencies are calculated with the Fast-J radiative transfer algorithm of *Wild et al.* [2000], which uses a seven-wavelength quadrature scheme and accounts accurately for Rayleigh scattering as well as Mie scattering by aerosols and clouds. A total of 52 photolysis reactions are included and photolysis calculations are performed every hour. Vertically resolved CODs and cloud fractions are taken from the GEOS meteorological archives with 6-hour resolution. To take into account the vertical subgrid variability of clouds (cloud overlap), we use

138 in this paper the Approximate Random Overlap (RAN) scheme unless explicitly stated. The
139 RAN scheme assumes that the grid average COD is

140 $$\tau_c' = \tau_c \cdot f^{3/2} \quad (1)$$

141 where τ_c is the COD in the cloudy portion of the grid and f is the cloud fraction in each layer
142 [*Briegleb*, 1992]. The column COD is the sum of τ_c' for each layer of the column. *Briegleb*
143 [1992] showed that RAN yields a reasonable approximation to a detailed random overlap
144 calculation for the heating rate. RAN is also a good approximation of the maximum-random
145 overlap, which is more computationally expensive, in terms of the radiative impact of clouds on
146 tropospheric chemistry [*Liu et al.*, 2006]. Because the linear scheme (LIN), where $\tau_c' = \tau_c \cdot f$, was
147 used for standard tropospheric chemistry simulations in all previous papers using GEOS-Chem,
148 we also present model results with LIN when quantifying the global mean radiative effects of
149 clouds (**Table 1**) for comparison purposes. Clouds are assumed to be fully scattering (i.e., cloud
150 single scattering albedo SSA=1.0). Monthly mean surface albedos are those of *Herman and*
151 *Celarier* (1997). The model uses climatological O_3 concentrations as a function of latitude,
152 altitude, and month to calculate the absorption of UV radiation by O_3. Using tropospheric O_3
153 concentrations from the model simulation (vs. climatology) has little effect on our results [*Liu et*
154 *al.*, 2006].

155 The radiative effects of clouds in the model are represented by subtraction of a clear-sky
156 simulation from a cloudy-sky simulation. In the clear-sky simulation CODs are set to zero in the
157 calculation of photolysis frequencies while other roles of clouds (i.e., transport, wet removal,
158 heterogeneous chemistry and lightning NO_x emissions associated with deep convective clouds)
159 are present in both the clear-sky and cloudy-sky simulations.

160 **3. Cloud Fields**

In this section, we describe briefly how clouds are formed, intercompare CODs in the three GEOS meteorological archives, and evaluate the model diagnosed CODs with global satellite observations. Since Fast-J requires as input the grid-scale COD in vertical model layers, the intercomparison and evaluation will help us understand the sensitivities of tropospheric chemistry to these cloud fields.

3.1. Cloud Formation

In GEOS1-STRAT, convective and large-scale cloudiness are diagnosed as part of the cumulus and large-scale parameterizations [*Takacs et al.*, 1994]. They are combined into random overlap (CLRO) and maximum overlap (CLMO) cloudiness. The total cloud fraction, f, at each level is then obtained by: $f = 1 - (1\text{-CLRO}) \cdot (1\text{-CLMO})$. CODs are specified based on cloud type and temperature. The "maximum overlap" clouds are assigned an optical depth of 16 per 100mb and the "random overlap" clouds are assigned an optical depth based on an empirical relation between local temperature and optical depth.

In GEOS-3, the occurrence of clouds is empirically diagnosed based on grid-scale relative humidity and subgrid-scale convection. For large-scale clouds, COD is empirically assigned values proportional to the diagnosed large-scale liquid water. For convective clouds, COD is prescribed as 16 per 100mb. A temperature-dependence is used to distinguish between water and ice clouds. The total optical depth in a given model layer is computed as a weighted average between the large-scale and subgrid scale optical depths, normalized by the total cloud fraction in the layer.

In GEOS-4 and its parent general circulation model fvGCM (finite-volume GCM), the physics was adopted from the NCAR CCM3 (Community Climate Model version 3) and WACCM (Whole Atmosphere Community Climate Model) with several modifications [*Kiehl et*

184 *al.*, 1998]. The cloud microphysics follows the simple diagnostic condensate parameterization in
185 the standard CCM3. The diagnosis of cloud fraction uses a modified *Slingo* [1987] scheme.
186 Cloud fraction depends on relative humidity, vertical velocity, atmospheric stability and
187 convective mass fluxes. The scheme diagnoses three types of cloud, i.e., low-level marine
188 stratus, convective cloud, and layered cloud. The parameterization of cloud optical properties is
189 described in *Kiehl et al.* [1998].

190 **3.2. Evaluation of GEOS Cloud Optical Depths with Satellite Observations**

191 Since information about the global climatology of the vertical distribution of cloud
192 water/ice content and optical depth is currently lacking, we focus on column CODs when
193 evaluating model cloud fields against the observations. Satellite retrieved products of column
194 CODs are available from the Moderate Resolution Imaging Spectroradiometer (MODIS)
195 [*Platnick et al.*, 2003] and the International Satellite Cloud Climatology Project (ISCCP)
196 [*Rossow et al.*, 1996; *Rossow and Schiffer*, 1999]. The standard ISCCP D2 data set [*Rossow et*
197 *al.*, 1996] reports as column CODs the averaged values of individual pixels with nonlinear
198 weights that preserve the average cloud albedo (the so-called "radiative mean CODs" [*Rossow et*
199 *al.*, 2002]), while storing linear averages of individual pixel values of optical depth (the so-called
200 "linear mean CODs" [*Rossow et al.*, 2002]) in the form of mean cloud water content. It is
201 important to note that ISCCP radiative mean CODs are about a factor of 2-3 smaller than the
202 linear mean CODs (W.B. Rossow, personal communication, 2004). The MODIS data set
203 provides linear mean CODs and geometric mean CODs, the latter being a proxy for radiative
204 mean CODs [*e.g.*, *Oreopoulos and Cahalan*, 2005].

205 We previously compared in *Liu et al.* [2006] GEOS-3 monthly (linear mean) CODs with
206 MODIS (MOD08_M3.004) and ISCCP (D2, linear mean) retrievals for the year of 2001. We

made a similar comparison between GEOS1-STRAT, GEOS-3, GEOS-4, MODIS (MOD08_M3.005) and ISCCP (D2) datasets for June (not shown). Both MODIS and ISCCP CODs show peaks in the tropics and at mid-latitudes in the Northern Hemisphere (NH) and the marine stratus region in the Southern Hemisphere (SH, ~50-60ºS). GEOS CODs show similar features, with GEOS1-STRAT and GEOS-4 CODs substantially lower than the satellite retrievals by factors of about 5 and 2, respectively. The GEOS CODs we used are diurnal averages, but they are almost identical (in a zonal mean sense) to the daytime averages. Although GEOS-3 CODs are closest to the satellite retrievals, GEOS-3 tends to overestimate CODs in the tropics and NH lower mid-latitudes (extending from the subtropics). MODIS and ISCCP retrievals show high CODs at high southern latitudes, presumably due to errors associated with COD retrievals over snow or ice cover. ISCCP seems to have a similar problem in the summer (NH) very high latitudes, though MODIS appears to do much better in this latter case. This comparison, however, did not take into account how clouds overlap in the vertical.

We improve the comparison between GEOS and satellite CODs by considering cloud overlap. MODIS and ISCCP observations of global cloudiness assume only a single cloud layer is present in a given pixel and therefore implicitly include the effects of cloud overlap. Since we use in this study the RAN cloud overlap scheme in our model standard simulation, we compare the GEOS effective column CODs under the RAN scheme with MODIS and ISCCP all-sky grid-box (radiative mean) CODs (**Figure 1a**). GEOS CODs are τ_c' values in equation (1) integrated in the vertical column. MODIS and ISCCP all-sky grid-box CODs are averages over both grid-box cloudy and clear areas with nonlinear weights that preserve the average cloud albedo, as derived in the **Appendix**.

MODIS radiative mean CODs are very close to those of ISCCP in the tropics while the former is somewhat larger at mid-latitudes. As with linear mean CODs (not shown), MODIS and ISCCP radiative mean CODs also show peaks in the tropics and mid-latitudes (**Figure 1a**). Relative to linear mean CODs, GEOS effective CODs under the RAN scheme (**Figure 1a**) have smaller magnitude with similar latitudinal variations. These CODs also differ substantially among the GEOS archives. In the tropics, GEOS-4 effective CODs are most close to MODIS and ISCCP radiative mean CODs; at mid-latitudes, GEOS-4 and GEOS-3 effective CODs appear to bracket MODIS and ISCCP radiative mean CODs.

Figure 1b shows the relevant zonal mean total cloud fractions. The MODIS MOD35 cloud-mask fraction (i.e., "Cloud_Fraction_Mean_Mean" in the Collection 5 processing stream) is very close to the ISCCP cloud fraction. Both are diurnal-mean cloud fractions. Note that the MOD35 *daytime*-mean cloud-mask fraction (not shown) is very close to the corresponding diurnal-mean fraction. This indicates that there is not a large diurnal variation, at least in the zonal means, and justifies the combination of diurnal-mean ISCCP cloud fractions and the daytime-mean ISCCP CODs in the ISCCP all-sky calculations for Figures 1a and 1b. Relative to total cloud fractions in GEOS1-STRAT and GEOS-4, those in GEOS-3 appear to better agree with ISCCP retrievals as well as total cloud fractions from the MOD35 cloud mask. A similar under-prediction of GEOS-4 zonal mean cloud fraction was reported by *Norris and da Silva* [2007] for January 2001.

Also shown in **Figure 1b** (thick solid line) is the MOD06 COD-retrieval cloud fraction ("Cloud_Fraction_Combined_FMean"**)**. This is the fraction of MODIS pixels classified as cloudy for the purposes of doing COD retrievals. This is the appropriate cloud fraction to use for MODIS all-sky COD calculations and the one used in **Figures 1a.** It is significantly smaller than

252 the cloud-mask fraction, because the MODIS COD retrieval algorithms are more selective than
253 the cloud mask in order to return accurate COD values. This increased selectivity tends to
254 remove dubiously cloudy pixels that tend to have very small COD values anyway, so does not
255 produce an underestimate of all-sky COD. This was verified against Collection 004 retrievals
256 (not shown), which were less selective, with higher cloud fractions, but produced all-sky CODs
257 similar to Collection 005 values.

258 Discrepancies between CODs in the three GEOS archives include not only their
259 magnitudes but vertical distributions. We intercompare in **Figure 2** the latitude-height cross
260 sections of monthly zonal mean effective cloud extinction coefficients (km^{-1}) and cloud fractions
261 in GEOS1-STRAT (1996), GEOS-3 (2001) and GEOS-4 (2001) for June. Clouds in GEOS-4 are
262 optically much thinner in the tropical upper troposphere compared to those in GEOS1-STRAT
263 and GEOS-3; the latter two cases exhibit more similar spatial (especially vertical) distributions.

264 The global distributions of GEOS1-STRAT, GEOS-3, and GEOS-4 monthly mean
265 column effective CODs are shown in **Figure 3** in comparison with MODIS and ISCCP all-sky
266 grid-box radiative mean CODs for March 2001 when frequent cyclogenesis occurred in the NH.
267 Note the smaller color scale for GEOS1-STRAT. Also shown in **Figure 3** are the probability
268 distribution functions (PDF) of global monthly mean column CODs in each dataset. CODs in all
269 GEOS archives show maxima in the tropics associated with deep convective clouds and at
270 midlatitudes associated with extratropical cyclones in the NH and marine stratiform clouds in the
271 SH. Despite the different magnitudes of column CODs among the three archives, their features in
272 the global distributions (i.e., maxima in the tropics and at midlatitudes) are consistent with those
273 in the MODIS and ISCCP cloud retrieval products. Their probability distribution functions

indicate that CODs in the range of 1-3 are mostly seen in all GEOS archives (except GEOS1-STRAT) as well as MODIS and ISCCP retrievals.

4. Sensitivity of Photolysis Frequencies to Cloud Optical Depths

In this section, we examine the sensitivity of the global impact of GEOS1-STRAT, GEOS-3, and GEOS-4 clouds on photolysis frequencies. We focus on $J(O^1D)$ and $J(NO_2)$, which are the most critical parameters for determining OH and O_3 concentrations [*Thompson and Stewart*, 1991].

Figure 4 shows the simulated percentage changes in the June monthly daily mean $J(O^1D)$ due to the radiative effects of clouds with GEOS1-STRAT, GEOS-3, and GEOS-4, respectively. With GEOS1-STRAT and GEOS-3, $J(O^1D)$ in the tropics is enhanced by up to ~10-15% above the high clouds, and reduced by up to ~5-10% (GEOS1-STRAT) and ~10-20% (GEOS-3) below. These enhancements (reductions) reflect the backscattering (attenuation) of solar UV radiation above (below) the deep convective clouds. Similar effects are also seen above and below the low-level clouds at NH and SH midlatitudes. Overall, GEOS1-STRAT and GEOS-3 yield similar patterns in terms of the regions of $J(O^1D)$ enhancements and reductions due to the radiative impact of clouds, reflecting their similar vertical distributions of clouds (**Figure 2**). However, relative to GEOS1-STRAT, GEOS-3 gives larger enhancements (reductions) above (below) the clouds because of larger CODs.

By contrast, with GEOS-4, $J(O^1D)$ is enhanced (by ~5-10%) in most of the tropical troposphere and is reduced (by ~5%) only near the surface (<~1km). The optically much thinner clouds in the tropical upper troposphere in GEOS-4 allow more solar UV radiation to penetrate through and be subsequently reflected by low-level thick clouds. The net changes in $J(O^1D)$ in

297 the tropical middle troposphere are determined by the competition between the radiative effects
298 of high and low clouds. Indeed, the optically thicker clouds in the tropical upper troposphere in
299 GEOS1-STRAT and GEOS-3 allow less solar UV radiation to penetrate down, resulting in net
300 reductions in the middle troposphere.

301 The sensitivity of $J(NO_2)$ to the three cloud fields is spatially similar to that of $J(O^1D)$ but
302 has a larger magnitude (not shown); the latter was discussed in *Liu et al.* [2006].

303

304 **5. Sensitivity of Key Oxidants to Cloud Optical Depths**

305 We examine in this section the sensitivity of OH and O_3 calculations to the CODs in the
306 three meteorological archives. Model results are discussed in terms of global means (section 5.1)
307 and monthly zonal means (section 5.2).

308 **5.1. Global Mean**

309 Shown in **Table 1** are the simulated percentage changes in the global mean concentrations
310 of key oxidants in the troposphere, photolysis frequencies and global mean lifetimes of
311 methylchloroform (CH_3CCl_3, MCF) and CH_4 due to the radiative effects of clouds with the
312 GEOS1-STRAT (1996), GEOS-3 (2001), and GEOS-4 (2001) meteorological archives for June
313 and January. Results with both RAN and LIN cloud overlap assumptions are shown; LIN was
314 used in previous standard versions of the GEOS-Chem model and the corresponding results are
315 presented here for comparison. With GEOS1-STRAT, calculated global mean changes in OH,
316 O_3, NO_x, HO_2, CH_2O, CO, $J(O^1D)$, $J(NO_2)$, and $J(CH_2O)$ for June are generally less than a few
317 percent, using either RAN or LIN. We found the same (i.e., less than ~6%) previously with
318 GEOS-3 [*Liu et al.*, 2006]. The slight differences between the model results for GEOS-3
319 reported in **Table 1** here and Table 2 of *Liu et al.* [2006] reflect an updated version of the model

used in this study. In January, both GEOS1-STRAT and GEOS-3 yield global mean changes that are still less than ~6% (RAN) or ~9% (LIN). As we discussed in section 4 and will discuss further below, the global mean effects are similar for these two meteorological archives because of their similar vertical distribution of clouds, even though their column CODs differ by a factor of about 5. The fact that the global mean effect remains modest when driven with GEOS1-STRAT or GEOS-3 reflects mainly an offsetting effect of above-cloud enhancements and below-cloud reductions.

GEOS-4 cloud perturbations to global mean OH concentrations and photolysis frequencies are much larger than occurs with either GEOS1-STRAT or GEOS-3, in particular when LIN is used for cloud overlap. For instance, global mean OH concentrations change by ~7% (RAN) or ~13% (LIN) due to the effects of clouds in GEOS-4 (versus <~2% change in GEOS1-STRAT and GEOS-3). This is surprising given that the column CODs in GEOS-4 are larger (smaller) than those in GEOS1-STRAT (GEOS-3) by a factor of ~2.5 (2). The larger global mean effect in our model with GEOS-4 results from the fact that optically thin upper-tropospheric clouds allow the (optically thick) lower-tropospheric clouds to have a large radiative effect. In other words, solar radiation can penetrate through the upper troposphere and is reflected by low-level thick clouds, increasing photochemical activity in most of the troposphere. Such large effects of clouds on OH were also seen in GEOS-Chem simulations driven by GISS GCM meteorological data, which has thick clouds in the tropical lower troposphere [*Wu et al.*, 2007]. On the other hand, with GEOS-4, the differences in cloud perturbations to global mean OH concentrations and photolysis frequencies due to the RAN and LIN assumptions used in the model are much larger than those with GEOS1-STRAT and GEOS-3. It is because the optically much thinner (thicker)

342 high clouds in GEOS-4 (GEOS1-STRAT and GEOS-3) enhance (reduce) the effect of different
343 assumptions about cloud overlap on the reflection from low clouds.

344 We calculated the lifetimes of MCF and CH_4, proxies for the global mean OH
345 concentrations. With GEOS1-STRAT or GEOS-3, the annual mean lifetime of MCF (CH_4)
346 increases by less than a few percent as a result of the radiative effects of clouds (**Table 1**). We
347 find that the MCF (CH_4) lifetime may increase even if global mean OH concentrations increase.
348 This is because the MCF-OH (CH_4-OH) reaction constant is temperature dependent and the
349 MCF (CH_4) lifetime is more sensitive to the OH concentrations in the lower troposphere (versus
350 the middle and upper troposphere) and the tropics (versus higher latitudes). With GEOS-4,
351 annual mean lifetimes of MCF and CH_4 decrease by 6% (RAN) or 11% (LIN) due to the effects
352 of clouds. As we will show below, this large decrease compared to that with GEOS1-STRAT or
353 GEOS-3 reflects the broader increases in OH concentrations in the free troposphere, including
354 the tropics, in the model with GEOS-4. The very large changes in the effects on MCF and CH4
355 lifetimes due to the RAN and LIN assumptions (i.e., -6% vs. -11%) are due to the large changes
356 in the effects on OH concentrations, as discussed above. One may note that even without clouds,
357 the MCF (CH4) lifetime in the simulation with GEOS-4 is significantly longer than that with
358 GEOS1-STRAT or GEOS-3. (hyl note: CH4 lifetime in GEOS-4 is ~12 years which is much
359 higher than 9.8 years previously reported by Wu et al. [2007]. My OH in GEOS-4 is too low. I'm
360 investigating this by re-running GEOS-4 simulations. GEOS-3 results agree with those of Wu et
361 al.)

362 **5.2. Zonal Mean**

363 **Figure 5** shows simulated percentage changes in monthly zonal mean OH and O_3 due to
364 the radiative effects of clouds for June when the model is driven by GEOS1-STRAT, GEOS-3

365 and GEOS-4, respectively. As with photolysis frequencies (**Figure 4**), the regions of OH
366 enhancements and reductions due to the radiative impact of clouds show similar patterns with
367 GEOS1-STRAT and GEOS-3 because of similar vertical distributions of clouds in the two
368 archives, although the magnitude of their respective relative changes in OH are different. In the
369 tropics, OH is enhanced by up to ~5% (GEOS1-STRAT) or ~5-10% (GEOS-3) above the deep
370 convective clouds, and reduced by ~5-10% (GEOS1-STRAT) or ~5-20% (GEOS-3) below,
371 reflecting the backscattering (attenuation) of solar radiation above (below) the clouds. At NH
372 midlatitudes, OH is enhanced by ~2-5% (GEOS1-STRAT) or ~5-10% (GEOS-3) above the low-
373 level clouds; at SH subtropics, OH is enhanced by ~5%; at SH high latitudes, the impact of
374 clouds on OH does not show consistent patterns. Near the surface, OH decreases by up to ~15-
375 35% because of clouds, with the largest percentage decreases occurring at midlatitudes. By
376 contrast, with GEOS-4, OH is enhanced (by ~5-10%) in most of the troposphere and is reduced
377 (by up to ~20%) only near the surface (<~1km). Again, enhanced OH in the tropical middle
378 troposphere is a result of the optically much thinner clouds in the tropical upper troposphere in
379 GEOS-4, allowing solar UV radiation to not only penetrate down but be reflected back by low-
380 level clouds.

381 With GEOS1-STRAT and GEOS-3, the maximum impact of clouds on O_3 (~2-5%) is seen
382 in the tropical upper troposphere with a trivial impact elsewhere (**Figure 5**, right panels). The
383 pattern of enhancements above clouds and reductions below clouds for OH are not seen for O_3,
384 partly reflecting the relatively long lifetime of O_3 and the short lifetime of OH. More
385 importantly, the tropical lower troposphere is overall a regime of net O_3 loss (~1 ppbv/day on
386 zonal average) due to a low NO_x environment; therefore, the radiative effects of tropical deep
387 convective clouds suppress this net O_3 loss (e.g., by a few percent with GEOS-3) primarily via

388 the reaction $O(^1D) + H_2O \rightarrow 2\ OH$, increasing O_3 in this part of the troposphere. On the other
389 hand, with GEOS-4, the overall impact of clouds on O_3 is small, with a maximum in the
390 middle/upper troposphere at NH high latitudes. We showed in *Liu et al.* [2006] that tropical
391 upper tropospheric O_3 is much less sensitive to the radiative effects of clouds in the GEOS-Chem
392 model (driven with GEOS-3) than previously reported by *Tie et al.* [2003] using the MOZART-2
393 model (~5% versus ~20-30%). Here we find that when driven with the other two meteorological
394 archives that feature either different magnitudes of column CODs or different vertical
395 distributions in the vertical, GEOS-Chem still shows much less sensitivity of tropospheric O_3 to
396 the radiative effects of clouds than does MOZART-2. Indeed, our result was quite comparable to
397 that of *Wild* [2007] who found a global O_3 burden change of 2.5% when all cloud cover was
398 removed in the FRSGC/UCI CTM. It appears, however, that global distributions of clouds in the
399 MOZART-2 model used by *Tie et al.* [2003] are similar to those in GEOS-4, both
400 underestimating the optical depth due to high clouds in the tropics. These suggest that differing
401 cloud fields including cloud vertical distributions cannot explain the majority of the
402 discrepancies between the results from GEOS-Chem and MOZART-2. A ~20-30% increase in
403 tropical upper tropospheric O_3 solely due to the radiative effects of clouds is unlikely, as we
404 previously argued [*Liu et al.*, 2006].
405
406 **6. Sensitivity to the Magnitude of Cloud Optical Depths**
407 Comparing the effects of clouds in GEOS1-STRAT and GEOS-3, which feature similar
408 vertical distribution of clouds, provides a sense of the sensitivity of simulated photolysis
409 frequencies and tropospheric oxidants to the magnitude of CODs. To see the full range of
410 sensitivity to COD magnitude, we examine in this section sensitivity simulations where the

411 magnitude of 3-D CODs is progressively adjusted. We choose GEOS-3 (versus GEOS-4) for
412 these perturbation experiments because its high clouds are optically thicker and probably more
413 realistic (section 3). These results should prove useful for understanding the radiative impact of
414 clouds in other models with similar vertical distributions of clouds. They will also help
415 understand how potential changes in the magnitude of CODs in a future climate may affect
416 tropospheric chemistry. To help understand the results from our sensitivity simulations for
417 different seasons, we first examine the seasonal and latitudinal variability in the distributions of
418 clouds and their effects on photolysis frequencies and tropospheric oxidants.

419 **Figure 6** shows the zonal mean latitude-height cross-sections of GEOS-3 monthly mean
420 cloud extinction coefficient (km^{-1}) for January, March, June and October. Vertical profiles of
421 monthly zonal mean cloud extinction coefficients at selected latitudes (46ºN, 38ºN, 30ºN,
422 equator, 30ºS, 38ºS, and 46ºS) are shown in **Figure 7** (0-16km) and **Figure 8** (0-3km),
423 respectively. In all months, GEOS-3 shows high clouds associated with deep convection in the
424 tropics and low-level stratiform clouds at middle and high latitudes. While the overall patterns of
425 cloud distributions are similar in different months, there are significant regional differences. In
426 the tropics, extinction coefficients have a local maximum in the upper troposphere in Jan, March
427 and June; they are more uniform in the upper and middle troposphere in October. In the
428 middle/high latitudes, the SH exhibits substantially larger extinction in the lower troposphere
429 than the NH does (**Figure 8**). These relative distributions of clouds will affect how photolysis
430 frequencies and tropospheric oxidants respond to the varying magnitude of CODs.

431 We show in **Figure 9** the model calculated percentage changes in monthly zonal mean
432 photolysis frequencies $J(O^1D)$ because of the radiative effects of clouds indicated in **Figures 7**
433 **and 8**. In the tropics, $J(O^1D)$ are enhanced above and reduced below about 7km (5km) in

January, March and June (October). In January, March and June, the local maximum in cloud extinction coefficients in the upper troposphere prevents solar UV radiation from penetrating down, leading to reductions in $J(O^1D)$ in more of the troposphere; this is particularly true for June. In October, the cloud extinction coefficients in the middle and upper troposphere are more uniformly distributed and the reflection from lower levels becomes more important, resulting in reductions in $J(O^1D)$ in less of the troposphere. In the SH, $J(O^1D)$ is enhanced in most of the troposphere except near the surface where it is reduced by ~10-30%. In the NH, by contrast, this transition from enhancement to reduction occurs at higher altitudes (~2-6km) in all seasons except June, reflecting higher and optically thicker clouds in the NH than in the SH during those seasons (**Figure 7**). In June, the NH exhibits decreased cloud extinction in the lower free troposphere (~1-2 km, **Figures 6 and 8**), allowing more solar radiation reflected back by boundary layer thick clouds. The impact of clouds on $J(NO_2)$ (not shown) is similar to that on $J(O^1D)$, but as discussed earlier, $J(NO_2)$ is more sensitive to the presence of clouds than $J(O^1D)$. The impact of clouds on OH concentrations at different latitudes and seasons (not shown) are similar to those on $J(O^1D)$ and $J(NO_2)$.

Figure 10 shows the model sensitivities of regional and global mean OH to the magnitude of CODs in January, March, June and October. $J(O^1D)$ and $J(NO_2)$ show similar sensitivities (not shown). Plotted are the percentage changes in global and column (at selected latitudes as indicated in **Figures 7-9**) mean OH relative to the standard simulation as the magnitudes of 3-D CODs are adjusted progressively from -100% to 100%. A -50% change in CODs corresponds to half of the original GEOS-3 CODs with the same 3-D spatial distributions. Global mean OH (solid line) is shown to have only modest changes at all CODs. Again, this reflects the opposite effects of enhanced (weakened) photochemistry above (below) clouds. It also reflects the overall

opposite effects of clouds in the NH and the SH. The slopes of the global mean curve indicate that global mean OH shows the strongest sensitivity to CODs at the low end. The slopes remain positive and decrease with increasing CODs during January and October; in contrast, the slopes change from positive to negative with increasing CODs during March and June. The decreasing slopes with increasing CODs reflect saturation at large CODs.

In January, March and October, the higher and optically thicker clouds in the NH (**Figures 6-8**) lead to a decreasing trend in OH as the CODs increase (**Figure 10**); the thinner clouds in the SH middle troposphere (**Figures 6-8**) allow solar radiation to be reflected by the low stratus clouds, resulting in an increasing trend in OH as the CODs increase (**Figure 10**). In June, OH is less sensitive to CODs than in other months (±4% versus ±15%) in both hemispheres. This reduced sensitivity is because boundary-layer clouds in GEOS-3 become optically thicker and mid-level clouds thinner in the NH while mid-level clouds become thicker at the SH mid-latitudes (**Figures 7-8**). The latter reflects enhanced frequency of mid-latitude cyclogenesis in the wintertime. Column mean OH concentrations at all latitudes show higher (lower) sensitivity at small (large) CODs.

We conclude that the modest effects of the perturbation to GEOS-3 CODs on global mean OH are due to the compensation between above-cloud enhancements and below-cloud reductions (in the vertical) and the opposite responses to this perturbation in the two hemispheres (in the horizontal). The effects would be larger if GEOS-4 cloud distributions were used in these perturbation experiments because of smaller compensations above and below clouds. Monotonic increases in global mean OH for January and October reflect the dominant backscattering from low-level clouds, while non-monotonic changes for March and June are a result of the sufficiently large optical depths due to high clouds which allow less solar radiation to penetrate

480 down to the lower levels and thus limit backscattering from low-level clouds. On the other hand,
481 global and regional column mean O_3 essentially increase monotonically when the CODs are
482 varied from -100% to 100%, but the effects of clouds remain modest (<5%) (not shown).
483
484 **7. Sensitivity to Cloud Absorption of Solar Radiation**
485 We present in this section a cautionary note that 0.99 is too low a value for cloud single
486 scattering albedo (SSA) and is not consistent with current knowledge of cloud absorption of solar
487 radiation at the ultraviolet wavelengths relevant to tropospheric chemistry. This unrealistic value
488 was cited in some recent literature of tropospheric chemistry [*e.g., Tie et al.*, 2003]. Pure water
489 clouds are inefficient absorbers and their SSAs are between 0.999990 and 0.999999 in the
490 ultraviolet wavelength range [*Hu and Stamnes*, 1993]. Even for contaminated clouds containing
491 black carbon, SSA is still between 0.999 and 0.9999 at 550nm [*Chylek et al.*, 1996]. Using a
492 SSA value as low as 0.99 would lead to large reductions in below-cloud actinic fluxes and thus
493 photolysis frequencies and to a lesser extent above the clouds.
494 We show in **Figure 11** the simulated percentage changes in the June monthly zonal mean
495 $J(O^1D)$, $J(NO_2)$ and OH due to the radiative effects of clouds (GEOS-3), using cloud SSA=0.99
496 (left panels) and SSA=0.999 (right panels), respectively. These plots can be compared to those
497 presented earlier in this paper (**Figure 4 and 5**) where SSA=1.0 was used in the standard cloudy-
498 sky simulation. Using SSA=0.99 is seen to significantly decrease the calculated radiative effects
499 of clouds, both below and above the clouds. We find that while a 1 per mil decrease in SSA
500 (from 1.0 to 0.999) leads to only ~1-2% decrease in $J(O^1D)$, $J(NO_2)$ and OH concentrations, 1%
501 decrease in SSA (from 1.0 to 0.99) would decrease photolysis frequencies and OH by ~5-10% in
502 most of the troposphere. This reflects the strong sensitivity of cloud transmittance and cloud

503 albedo to cloud absorption. Similar calculations with GEOS-4 indicate smaller effects,
504 suggesting in this case the magnitude of CODs is more important than the vertical distribution. In
505 a word, caution should be exercised not to use for cloud SSA a value lower than 0.999 (e.g.,
506 0.99) in model simulations of tropospheric chemistry.
507
508 **8. Summary and Conclusions**
509 We have examined the sensitivity of photolysis frequencies and key tropospheric
510 oxidants to cloud vertical distributions and optical properties in terms of the radiative effects of
511 clouds in a global 3-D CTM (GEOS-Chem) coupled with the Fast-J radiative transfer algorithm.
512 The model was driven with a series of meteorological archives (GEOS1-STRAT, GEOS-3 and
513 GEOS-4) generated by the GEOS DAS at the NASA GMAO, which have significantly different
514 cloud optical depths (CODs) and vertical distributions. An approximate random overlap (RAN)
515 scheme was used to take into account the vertical subgrid variability of cloudiness (cloud
516 overlap). The radiative effects of clouds in the model are represented by subtraction of a zero-
517 CODs simulation from the standard (cloudy-sky) simulation. Our objective was to improve our
518 understanding of the role that different cloud fields played in the variability of tropospheric
519 oxidants among global models in terms of the radiative effects of clouds on tropospheric
520 chemistry.
521 We intercompared the GEOS effective column CODs under the RAN scheme and
522 evaluated them with the satellite retrieval products of radiative mean CODs from the Moderate
523 Resolution Imaging Spectroradiometer (MODIS) and the International Satellite Cloud
524 Climatology Project (ISCCP). All CODs show peaks in the tropics associated with deep
525 convective clouds and at midlatitudes associated with extratropical cyclones in the Northern

526 Hemisphere (NH) and marine stratiform clouds in the Southern Hemisphere (SH). However,
527 CODs differ substantially among the GEOS archives. In the tropics, GEOS-4 effective CODs are
528 most close to MODIS and ISCCP radiative mean CODs; at mid-latitudes, GEOS-4 and GEOS-3
529 effective CODs appear to bracket MODIS and ISCCP radiative mean CODs. With respect to
530 vertical distribution, clouds in GEOS-4 are optically much thinner in the tropical upper
531 troposphere compared to those in GEOS1-STRAT and GEOS-3.

532 By examining the sensitivity of photolysis frequencies and tropospheric oxidants, with a
533 focus on $J(O^1D)$, $J(NO_2)$, OH and O_3, to the three GEOS cloud fields, we illustrated that the
534 radiative impact of clouds on global tropospheric chemistry is more sensitive to cloud vertical
535 distribution than to the magnitude of column COD. Specifically, our model calculations indicate
536 that the changes in global mean OH ($J(O^1D)$, $J(NO_2)$) due to the radiative effects of clouds in
537 June are about 0.0% (0.4%, 0.9%), 0.8% (1.7%, 3.1%), and 7.3% (4.1%, 6.0%), for GEOS1-
538 STRAT, GEOS-3 and GEOS-4, respectively. It is important to note that the distribution of
539 photolysis frequencies and OH concentrations shows much larger changes than global mean
540 values do. For instance, maximum decreases in OH concentrations of ~15-35% occur near the
541 midlatitude surface. The effects on global mean OH are similar for GEOS1-STRAT and GEOS-3
542 due to their similar vertical distributions of clouds, even though the column CODs in the two
543 archives differ by a factor of about 5. Despite a factor of 2 smaller optical depths than those
544 clouds in GEOS-3, clouds in GEOS-4 have a much larger impact on global mean photolysis
545 frequencies and OH. The reason is that with GEOS-4, more solar UV radiation is able to
546 penetrate through the optically thin clouds in the upper troposphere, increasing backscattering
547 from low-level clouds and leading to enhanced photochemical activity through most of the free

548 troposphere. The net effects of clouds in the middle troposphere are largely determined by the
549 competition between the radiative effects of high and low clouds.

550 With each of the three (GEOS1-STRAT, GEOS-3, and GEOS-4) cloud distributions, the
551 model global burden of O_3 changes by only a few percent (<5%) as a result of radiative
552 perturbations from clouds, consistent with the result of *Wild* [2007]. In all cases, tropical upper
553 tropospheric O_3 is much less sensitive to the radiative effects of clouds than previously reported
554 by *Tie et al.* [2003] who used the MOZART-2 model (~5% versus ~20-30%). We argue that
555 differing cloud vertical distributions and optical depths, if present, cannot explain the majority of
556 the discrepancies between the GEOS-Chem and MOZART models.

557 We performed model perturbation experiments to see the full range of the sensitivities of
558 photolysis frequencies and tropospheric oxidants to CODs with varying magnitudes. The model
559 driven by GEOS-3 predicts only modest changes in global mean OH concentrations when the
560 magnitudes of 3-D CODs are progressively varied by -100% to 100% without altering cloud
561 spatial distributions. It reflects the compensating effect between above-cloud enhancements and
562 below-cloud reductions as well as the overall opposite responses to the cloud perturbation in the
563 NH and the SH. The latter was because in most of the year the NH has clouds that are higher and
564 optically thicker while the SH has thinner (thicker) clouds in the middle (lower) troposphere.
565 Global mean OH shows the strongest sensitivity at the small end of CODs and becomes more or
566 less saturated at the large end. On the other hand, the effects of clouds on global burden of O_3 in
567 these perturbation experiments remain modest (<5%).

568 Caution should be exercised not to use a value for cloud single scattering albedo (SSA)
569 lower than 0.999 in order to be consistent with the current knowledge of cloud absorption at the
570 ultraviolet wavelengths relevant to tropospheric photochemistry. Realistic values for cloud SSA

571 are between 0.999 and 1.0. Moreover, the calculated radiative effects of clouds are very sensitive
572 to the specified cloud SSA. Using 0.99 for cloud SSA in our model driven by GEOS-3 would
573 decrease simulated $J(O^1D)$, $J(NO_2)$, and OH concentrations by ~5-10% in most of the
574 troposphere, relative to SSA=1.0.

575 Results from our sensitivity studies are robust with respect to varying cloud distributions
576 and optical depths and have important implications for model intercomparisons and for climate
577 feedback on tropospheric photochemistry. First, cloud vertical distributions and optical depths
578 often vary from model to model and may contribute substantially to the model-model
579 discrepancies in tropospheric OH (oxidation capability). While the differing magnitudes of
580 column CODs may explain part of this discrepancy, the differing vertical distribution of clouds
581 plays a more important role. Thus the impact of errors in the magnitude of CODs on simulated
582 OH concentrations is smaller than that of errors in the vertical distribution of clouds of similar
583 magnitude. Second, properly representing the vertical distribution of clouds in climate models
584 and its response to climate change is more important for predicting the feedback of cloud
585 changes in a warmer climate on tropospheric photochemistry. This requires an improved
586 representation of clouds, especially their vertical distribution, in current climate models. It is
587 made possible by the launchings of CloudSat and CALIPSO satellites (April 2006) where a
588 unique dataset of not only cloud optical and physical properties but also their vertical
589 distributions will be available for evaluating and constraining the models.

590

591 *Acknowledgments.* This work was supported by NASA Langley Research Center. Thanks are
592 due to Jennifer Logan (Harvard University) for discussions that inspired part of this work,
593 Bernhard Mayer (Institute of Atmospheric Physics of DLR, Germany) for discussions regarding

the cloud single scattering albedo, Yan Feng (University of California at San Diego) for communications about the effect of cloud overlap on photolysis frequencies, and Mat Evans (University of Leeds, UK) for his comments on an earlier manuscript. MODIS and ISCCP products are distributed by NASA Goddard Level 1 and Atmosphere Archive and Distribution System (http://ladsweb.nascom.nasa.gov) and Langley Atmospheric Sciences Data Center, respectively. The GEOS-Chem model is managed by the Atmospheric Chemistry Modeling Group at Harvard University with support from the NASA Atmospheric Chemistry Modeling and Analysis Program (ACMAP). The views, opinions, and findings contained in this report are those of the authors and should not be construed as an official NASA, NOAA or U.S. government position, policy, or decision.

Appendix. Derivation of MODIS and ISCCP all-sky grid-box cloud optical depths

The albedo (R_c) of a non-absorbing, horizontally homogeneous cloud is given by the two-stream approximation [*Lacis and Hansen*, 1974; *Seinfeld and Pandis*, 1998] as

$$R_c = \frac{\sqrt{3}(1-g)\tau_c}{2+\sqrt{3}(1-g)\tau_c} \tag{2}$$

where τ_c is in-cloud optical depth (COD) and g is the asymmetry factor. Assuming the value of g for cloud drops of radius much greater than the wavelength of visible light is 0.85, the above equation becomes

$$R_c = \frac{\tau_c}{\tau_c + 7.7} \tag{3}$$

Therefore, with the average cloud albedo preserved, MODIS or ISCCP grid-box mean cloud albedo (R_c') can be expressed as

$$R_c' = \frac{\tau_c'}{\tau_c'+7.7} = f \cdot \frac{\tau_c}{\tau_c + 7.7} \tag{4}$$

where τ_c' is *all-sky* grid-box radiative mean COD and f grid-box cloud fraction. Solving (4) for τ_c', we have

$$\tau_c' = \frac{f\tau_c \cdot 7.7}{(1-f)\tau_c + 7.7} \quad , \tag{5}$$

where the unprimed τ_c is the in-cloud radiative mean COD (the proxy geometric mean COD in the case of MODIS) for the region and period under consideration.

References

Bey I., D. J. Jacob, R. M. Yantosca, J. A. Logan, B. Field, A. M. Fiore, Q. Li, H. Liu, L. J. Mickley, and M. Schultz (2001), Global modeling of tropospheric chemistry with assimilated meteorology: Model description and evaluation, *J. Geophys. Res., 106*, 23,073-23,096.

Bloom, S., A. da Silva, D. Dee, M. Bosilovich, J.-D. Chern, S. Pawson, S. Schubert, M. Sienkiewicz, I. Stajner, W.-W. Tan, and M.-L. Wu (2005). Documentation and Validation of the Goddard Earth Observing System (GEOS) Data Assimilation System - Version 4. *Technical Report Series on Global Modeling and Data Assimilation* (Editor Max J. Suarez), NASA/TM-2005-104606, Vol. 26, NASA Goddard Space Flight Center, Greenbelt, Maryland, April.

Briegleb, B.P. (1992), Delta-Eddington approximation for solar radiation in the NCAR Community Climate Model, *J. Geophys. Res., 97*, 7603-7612.

Chylek, P., et al. (1996), Black carbon and absorption of solar radiation by clouds, *J. Geophys. Res., 101*, 23,365-23,371.

Crawford, J.H., D. Davis, G. Chen, R. Shetter, M. Muller, J. Barrick, and J. Olson (1999), An assessment of cloud effects on photolysis rates: Comparison of experimental and theoretical values, *J. Geophys. Res., 104*, 5725-5734.

Evans, M.J., and D.J. Jacob (2005), Impact of new laboratory studies of N_2O_5 hydrolysis on global model budgets of tropospheric nitrogen oxides, ozone, and OH, *Geophys. Res. Lett., 32*, L09813, doi:10.1029/2005GL022469.

Feng, Y., J.E. Penner, S. Sillman, and X. Liu (2004), Effects of cloud overlap in photochemical models, *J. Geophys. Res., 109*, D04310, doi:10.1029/2003JD004040.

Heald, C.L., D.J. Jacob, R.J. Park, B. Alexander, T.D. Fairlie, D.A. Chu, and R.M. Yantosca (2006), Transpacific transport of Asian anthropogenic aerosols and its impact on surface air quality in the United States, *J. Geophys. Res.***,** *111,* D14310, doi:10.1029/2005JD006847.

Herman, J.R., and E.A. Celarier (1997), Earth surface reflectivity climatology at 340-380 nm from TOMS data, *J. Geophys. Res., 102*, 28,003-28,011.

Hu, Y.X., and K. Stamnes (1993), An accurate parameterization of the radiative properties of water clouds suitable for use in climate models, *J. Climate, 6*, 728-742.

Intergovernmental Panel on Climate Change (IPCC) (2001), *Climate Change (2001): The Scientific Basis*, Cambridge University Press, UK.

Intergovernmental Panel on Climate Change (IPCC) (2007), *Climate Change (2007): The Scientific Basis*, Cambridge University Press, UK.

Kiehl, J.T., et al. (1998), The National Center for Atmospheric Research Community Climate Model: CCM3, *J. Climate, 11*, 1131-1150.

Krol, M.C., and M. van Weele (1997), Implications of variations in photodissociation rates for global tropospheric chemistry, *Atmos. Environ., 31*, 1257-1273.

Lacis, A.A., and J.E. Hansen (1974), A parameterization of the absorption of solar radiation in the Earth's atmosphere, *J. Atmos. Sci., 31*, 118-133.

Lefer, B.L., R.E. Shetter, S.R. Hall, J.H. Crawford, and J.R. Olson (2003), Impact of clouds and aerosols on photolysis frequencies and photochemistry during TRACE-P: 1. Analysis using radiative transfer and photochemical box models, *J. Geophys. Res., 108*(D21), 8821, doi:10.1029/2002JD003171.

Liu, H., J.H. Crawford, R.B. Pierce, P. Norris, S.E. Platnick, G. Chen, J.A. Logan, R.M. Yantosca, M.J. Evans, C. Kittaka, Y. Feng, and X. Tie (2006), Radiative effect of clouds on

tropospheric chemistry in a global three-dimensional chemical transport model, *J. Geophys. Res., 111*, doi:10.1029/2005JD006403.

Mao, H., W.-C. Wang, X.-Z., Liang, and R.W. Talbot (2003), Global and seasonal variations of O_3 and NO_2 photodissociation rate coefficients, *J. Geophys. Res., 108*(D7), 4216, doi:10.1029/2002JD002760.

Martin, R.V., D.J. Jacob, J.A. Logan, I. Bey, R.M. Yantosca, A.C. Staudt, Q. Li, A.M. Fiore, B.N. Duncan, H. Liu, P. Ginoux, and V. Thouret (2002), Interpretation of TOMS observations of tropical tropospheric ozone with a global model and in-situ observations, *J. Geophys. Res., 107*, 4351, doi:10.1029/2001JD001480.

Martin, R.V., C.E. Sioris, K. Chance, T.B. Ryerson, T.H. Bertram, P.J. Wooldridge, R.C. Cohen, J.A. Neuman, A. Swanson, and F.M. Flocke (2006), Evaluation of space-based constraints on global nitrogen oxide emissions with regional aircraft measurements over and downwind of eastern North America, *J. Geophys. Res.***,** *111*, D15308, doi:10.1029/2005JD006680.

McLinden, C.A., S.C. Olsen, B. Hannegan, O. Wild, M.J. Prather, and J. Sundet (2000), Stratospheric ozone in 3-D models: A simple chemistry and the cross-tropopause flux, *J. Geophys. Res., 105*, 14,653-14,665.

Norris, P. M., and A. M. da Silva (2007), Assimilation of satellite cloud data into the GMAO Finite-Volume Data Assimilation System using a parameter estimation method. Part I: Motivation and algorithm description, *J. Atmos. Sci., 64*, 3880-3895.

Oreopoulos, L., and R. F. Cahalan (2005), Cloud inhomogeneity from MODIS. *J. Climate, 18*, 5110–5124.

Park R. J., D. J. Jacob, B. D. Field, R. M. Yantosca, M. Chin (2004), Natural and transboundary pollution influences on sulfate-nitrate-ammonium aerosols in the United States: Implications for policy, *J. Geophys. Res., 109*, D15204, doi:10.1029/2003JD004473.

Platnick, S., M.D. King, S.A. Ackerman, W.P. Menzel, B.A. Baum, J.C. Riedi, and R.A. Frey (2003), The MODIS cloud products: Algorithms and examples from Terra, *IEEE Transactions on Geoscience and Remote Sensing, 41*(2), 459-473.

Quante, M. (2004), The role of clouds in the climate system, *J. Phys. IV France, 121*, 61-86.

Rossow, W.B., and R.A. Schiffer (1999), Advances in understanding clouds from ISCCP. *Bull. Am. Meteorol. Soc.*, *80*, 2261-2287.

Rossow, W.B., A.W. Walker, D.E. Beuschel, and M.D. Roiter (1996), *International Satellite Cloud Climatology Project (ISCCP) documentation of new cloud datasets*, Int. Counc. Of Sci. Unions, Paris, January.

Rossow, W.B., C. Delo, and B. Cairns (2002), Implications of the observed mesoscale variations of clouds for the Earth's radiation budget, *J. Climate, 15*, 557-585.

Seinfeld, J.H., and S.N. Pandis (1998), *Atmospheric Chemistry and Physics: From Air Pollution to Climate Change*, 1173-1174, pp.1326, John Wiley & Sons, Inc., New York.

Slingo, J.M. (1987), The development and verification of a cloud prediction scheme for the ECMWF model, *Quart. J. Roy. Meteor. Soc., 113*, 899-927.

Stephens, G.L. (2005), Cloud feedbacks in the climate system: A critical review, *J. Climate, 18*, 237-273.

Takacs, L.L., A. Molod, and T. Wang (1994), Documentation of the Goddard Earth Observing System (GEOS) general circulation model – version 1, *NASA Tech. Memo., TM-104606, 1*.

Tang, Y., et al. (2003), Impacts of aerosols and clouds on photolysis frequencies and photochemistry during TRACE-P: 2. Three-dimensional study using a regional chemical transport model, *J. Geophys. Res.*, *108*, 8822, doi:10.1029/2002JD003100.

Thompson, A.M. (1984), The effect of clouds on photolysis rates and ozone formation in the unpolluted troposphere, *J. Geophy. Res., 89*, 1341-1349.

Thompson, A.M., and R.W. Stewart (1991), Effect of chemical kinetics uncertainties on calculated constituents in a tropospheric photochemical model, *J. Geophys. Res., 96*, 13,089-13,108.

Thompson, A.M. (1992), The oxidizing capacity of the Earth's atmosphere – Probable past and future changes, *Science, 256*, 1157-1165.

Tie, X., S. Madronich, S. Walters, R. Zhang, P. Rasch, and W. Collins (2003), Effect of clouds on photolysis and oxidants in the troposphere, *J. Geophys. Res., 108*(D20), 4642, doi:10.1029/2003JD003659.

Wild, O. (2007), Modelling the global tropospheric ozone budget: exploring the variability in current models, *Atmos. Chem. Phys., 7*, 2643-2660.

Wild, O., X. Zhu, and M.J. Prather (2000), Fast-J: Accurate simulation of in- and below-cloud photolysis in tropospheric chemical models, *J. Atmos. Chem., 37*, 245-282.

Wu, S., L.J. Mickley, D.J. Jacob, J.A. Logan, R.M. Yantosca, and D. Rind (2007), Why are there large differences between models in global budgets of tropospheric ozone? *J. Geophys. Res., 112*, D05302, doi:10.1029/2006JD007801.

Yang, H., and H. Levy (2004), Sensitivity of photodissociation rate coefficients and O_3 photochemical tendencies to aerosols and clouds, *J. Geophys. Res., 109*(D24), D24301, doi: 10.1029/2004JD005032.

Zhang, M.H., et al. (2005), Comparing clouds and their seasonal variations in 10 atmospheric general circulation models with satellite measurements, *J. Geophys. Res., 110*, D15S02, doi:10.1029/2004JD005021.

Table 1. Simulated Percentage Changes in the Global Mean Concentrations of Tropospheric Chemical Species, Photolysis Frequencies and Global Mean Lifetimes of Methylchloroform (MCF) and CH_4 Due to the Radiative Effects of Clouds with Different Cloud Overlap Assumptions (RAN and LIN) in June and January[a], Following Table 4 of *Tie et al.* [2003] and Table 2 of *Liu et al.* [2006].

	GEOS1-STRAT (1996)		GEOS-3 (2001)		GEOS-4 (2001)	
Quantity[b]	RAN	LIN	RAN	LIN	RAN	LIN
			June			
OH	0.00	-0.73	0.80	2.05	7.26	12.63
O_3[c]	1.68	3.01	3.20	5.22	0.90	1.39
NO_x[d]	1.65	2.88	3.95	6.35	1.35	2.29
HO_2	-1.25	-2.27	-1.62	-2.29	0.82	1.48
CH_2O	0.54	1.38	1.73	3.32	-0.65	-0.98
CO	-0.33	0.11	-0.06	-0.36	-4.50	-7.50
$J(O^1D)$	0.40	-0.06	1.73	3.25	4.08	7.32
$J(NO_2)$	0.85	0.85	3.11	5.90	5.96	10.40
$J(CH_2O)$	0.72	0.70	2.70	5.18	4.93	8.73
			January			
OH	0.98	0.91	2.95	5.16	7.66	13.37
O_3[c]	1.45	2.61	1.91	3.39	0.87	1.37
NO_x[d]	1.01	1.68	3.89	5.86	2.43	3.72
HO_2	-0.62	-1.22	-0.71	-1.00	0.99	1.79
CH_2O	0.71	1.54	1.49	2.61	-0.57	-1.00
CO	0.07	0.61	-0.16	-0.37	-3.28	-5.59
$J(O^1D)$	1.43	1.62	4.00	6.58	4.89	8.59
$J(NO_2)$	1.81	2.32	5.72	9.43	7.14	12.06
$J(CH_2O)$	1.66	2.14	5.10	8.52	6.03	10.33
T (MCF)[e]	1.00 (6.22)[f]	2.77 (6.33)	0.78 (6.68)	0.53 (6.66)	-6.47 (7.36)	-10.91 (7.02)

T (CH_4)[e]	1.11 (10.50)[f]	2.97 (10.70)	1.01 (11.25)	0.90 (11.23)	-6.40 (12.35)	-10.80 (11.77)

[a]The radiative effects of clouds is represented by subtraction of the clear-sky (zero cloud optical depths) simulation from the cloudy-sky simulation.

[b]Global mean concentrations are calculated by dividing the global total moles of a species by those of air. Global mean photolysis frequencies are volume-weighted values. Thermal tropopause is locally diagnosed using the World Meteorological Organization (WMO) definition of tropopause.

[c]Actually the extended odd oxygen family defined as $O_x = O_3 + NO_2 + 2 \times NO_3 +$ peroxyacylnitrates + $HNO_4 + 3 \times N_2O_5 + HNO_3$.

[d]$NO_x \equiv NO + NO_2$.

[e]Percentage changes in global annual mean lifetimes of MCF and CH_4. The lifetimes are derived as the ratio of the total burden of atmospheric MCF or CH_4 to the tropospheric loss rate against oxidation by OH.

[f]Values in the parentheses indicate global annual mean lifetimes (years) of MCF and CH_4 under cloudy conditions.

Figure Captions

Figure 1. (a). GEOS1-STRAT (1996), GEOS-3 (2001) and GEOS-4 (2001) monthly zonal mean effective column cloud optical depths as a function of latitude are compared to MODIS (MOD08_M3.005, level-3 monthly global product at 1°×1° resolution) and ISCCP (D2, 280 km equal-area grid) retrievals (all-sky radiative mean) for June 2001. The Approximate Random Overlap (RAN, equation 1) is used to calculate GEOS effective column cloud optical depths. (b). June 2001 GEOS zonal mean total cloud fractions as a function of latitude, compared to ISCCP retrievals (thin black line) and MODIS retrievals (thick black lines — the dashed line is the MOD35 diurnal-average cloud mask and the solid line is the MOD06 COD-retrieval cloud fraction). Zonal means are calculated for MODIS and ISCCP data if there are less than 10% missing values over the longitudes. See text for details.

Figure 2. Latitude-height cross-sections of monthly zonal mean cloud extinction coefficient (left panels) and cloud fraction (right panels) for June in GEOS1-STRAT (1996), GEOS-3 (2001), and GEOS-4 (2001), respectively. The Approximate Random Overlap (RAN) is used to obtain GEOS grid-box effective cloud optical depths (equation 1). See text for details.

Figure 3. The global distributions of GEOS1-STRAT (1996), GEOS-3 (2001), and GEOS-4 (2001) monthly mean column effective cloud optical depths (left panels) are compared to MODIS and ISCCP retrievals (radiative mean) for March 2001. Note the smaller color scale for GEOS1-STRAT. The Approximate Random Overlap (RAN, see equation 1) is used to calculate GEOS column effective cloud optical depths. MODIS and ISCCP all-sky grid-box mean cloud

optical depths are averages over both cloudy and clear regions with nonlinear weights that preserve the average cloud albedo (equation 5). Also shown are the probability distribution functions (PDF) of global monthly mean cloud optical depths in each dataset (right bottom panel). See text for details.

Figure 4. Percentage changes in monthly zonal mean $J(O^1D)$ in the troposphere due to the radiative effects of clouds in June, as simulated by the GEOS-Chem model driven with GEOS1-STRAT (1996), GEOS-3 (2001) and GEOS-4 (2001), respectively. Filled contour levels are -50, -30, -20, -10, -5, -2, 0, 2, 5, 10, 20%. Dotted contours indicate negative changes.

Figure 5. Same as Figure 4, but shown for OH and O_3 concentrations. Contour levels are -50, -30, -20, -10, -5, -2, 0, 2, 5, 10, 20%. Dotted contours indicate negative changes.

Figure 6. Zonal mean latitude-height cross-sections of GEOS-3 monthly mean cloud extinction coefficient (km^{-1}) for January, March, June and October 2001.

Figure 7. Same as Figure 6, but shown as vertical profiles of monthly zonal mean cloud extinction coefficients (km^{-1}) at selected latitudes (46ºN, 38ºN, 30ºN, equator, 30ºS, 38ºS, and 46ºS) for January, March, June and October 2001. Also shown are averages over all latitudes (solid lines). Vertical profiles between the surface and 3 km where cloud extinction coefficients may exceed 1.0 km^{-1} are shown in Figure 8.

Figure 8. Same as Figure 7, but for the altitudes of 0-3 km.

Figure 9. Same as Figure 7, but for percentage changes in monthly zonal mean J(O^1D) due to the radiative effects of clouds.

Figure 10. Sensitivities of mean tropospheric OH concentrations to the magnitude of cloud optical depths in January, March, June and October, as simulated by the GEOS-Chem model driven with GEOS-3 (2001). Plotted in the figure are the percentage changes in global (solid lines) and column (at selected latitudes, dot and dashed lines) mean OH relative to the standard simulation as the magnitude of 3-D cloud optical depths is adjusted progressively from -100% to 100%. A -50% change in cloud optical depths corresponds to half of the original GEOS-3 cloud optical depth with the same 3-D spatial distributions.

Figure 11. Simulated percentage changes in the June monthly zonal mean J(O^1D), J(NO_2) and OH due to the radiative effects of clouds (GEOS-3, 2001), using cloud SSA=0.99 (left panels) and SSA=0.999 (right panels), respectively.

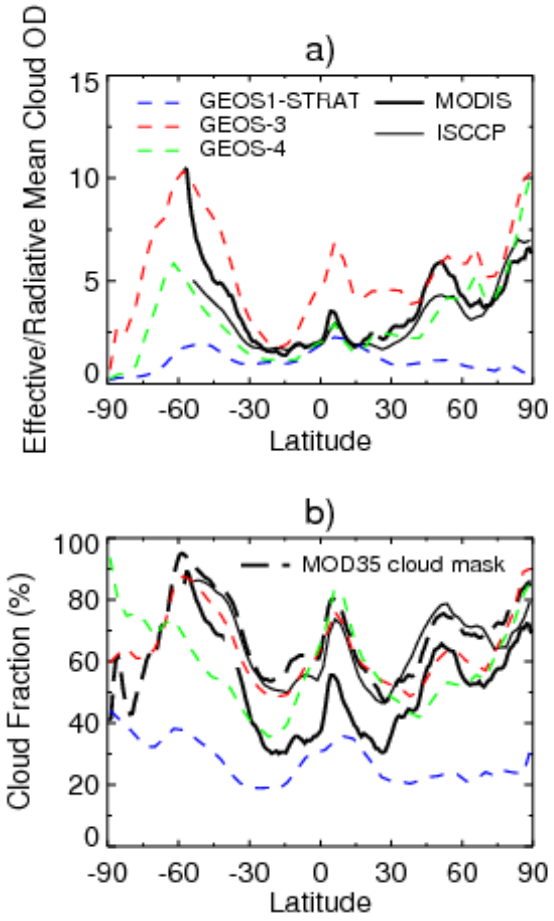

Figure 1. (a). GEOS1-STRAT (1996), GEOS-3 (2001) and GEOS-4 (2001) monthly zonal mean effective column cloud optical depths as a function of latitude are compared to MODIS (MOD08_M3.005, level-3 monthly global product at 1°×1° resolution) and ISCCP (D2, 280 km equal-area grid) retrievals (all-sky radiative mean) for June 2001. The Approximate Random Overlap (RAN, equation 1) is used to calculate GEOS effective column cloud optical depths. (b). June 2001 GEOS zonal mean total cloud fractions as a function of latitude, compared to ISCCP retrievals (thin black line) and MODIS retrievals (thick black lines — the dashed line is the MOD35 diurnal-average cloud mask and the solid line is the MOD06 COD-retrieval cloud fraction). Zonal means are calculated for MODIS and ISCCP data if there are less than 10% missing values over the longitudes. See text for details.

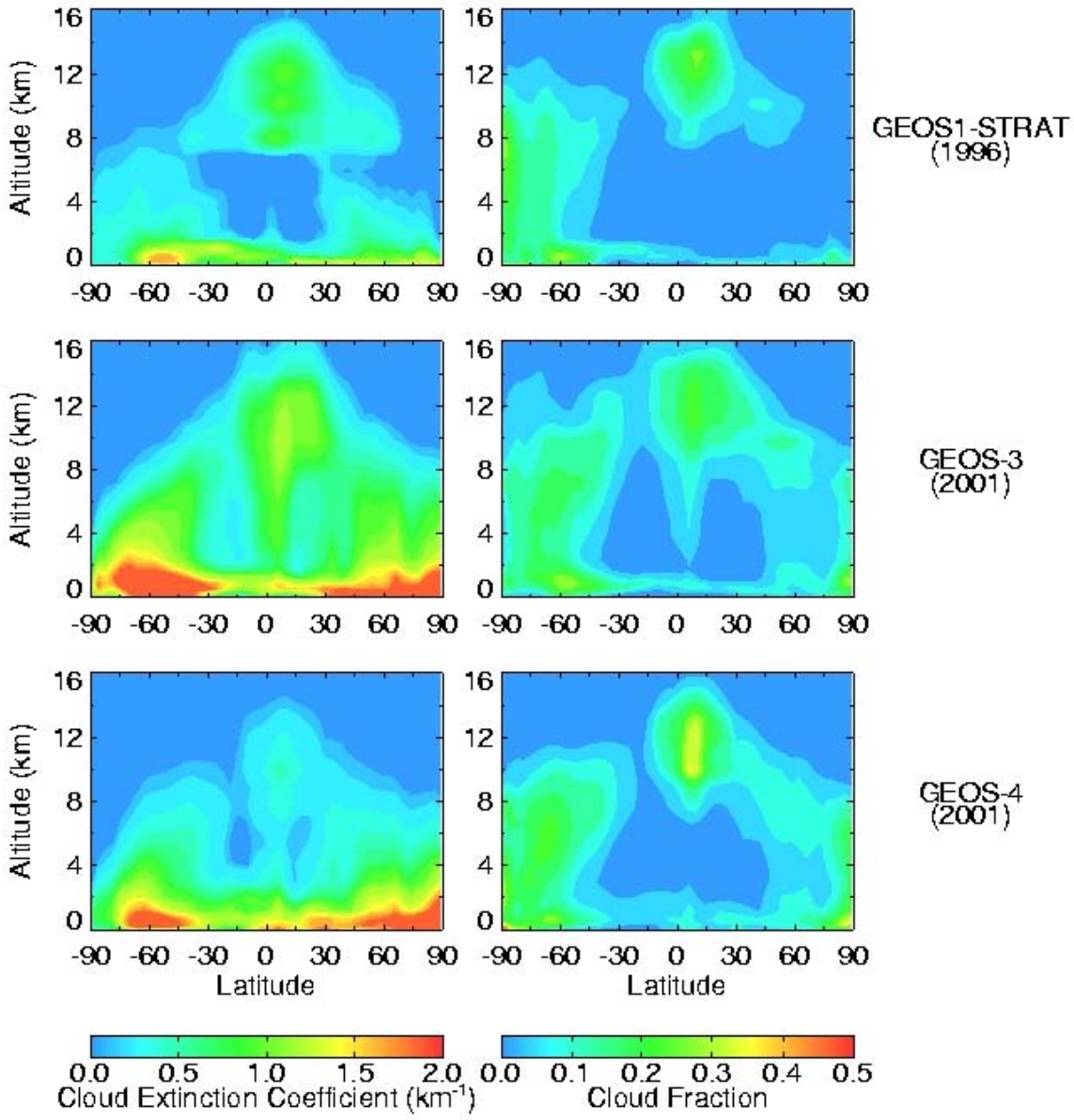

Figure 2. Latitude-height cross-sections of monthly zonal mean cloud extinction coefficient (left panels) and cloud fraction (right panels) for June in GEOS1-STRAT (1996), GEOS-3 (2001), and GEOS-4 (2001), respectively. The Approximate Random Overlap (RAN) is used to obtain GEOS grid-box effective cloud optical depths (equation 1). See text for details.

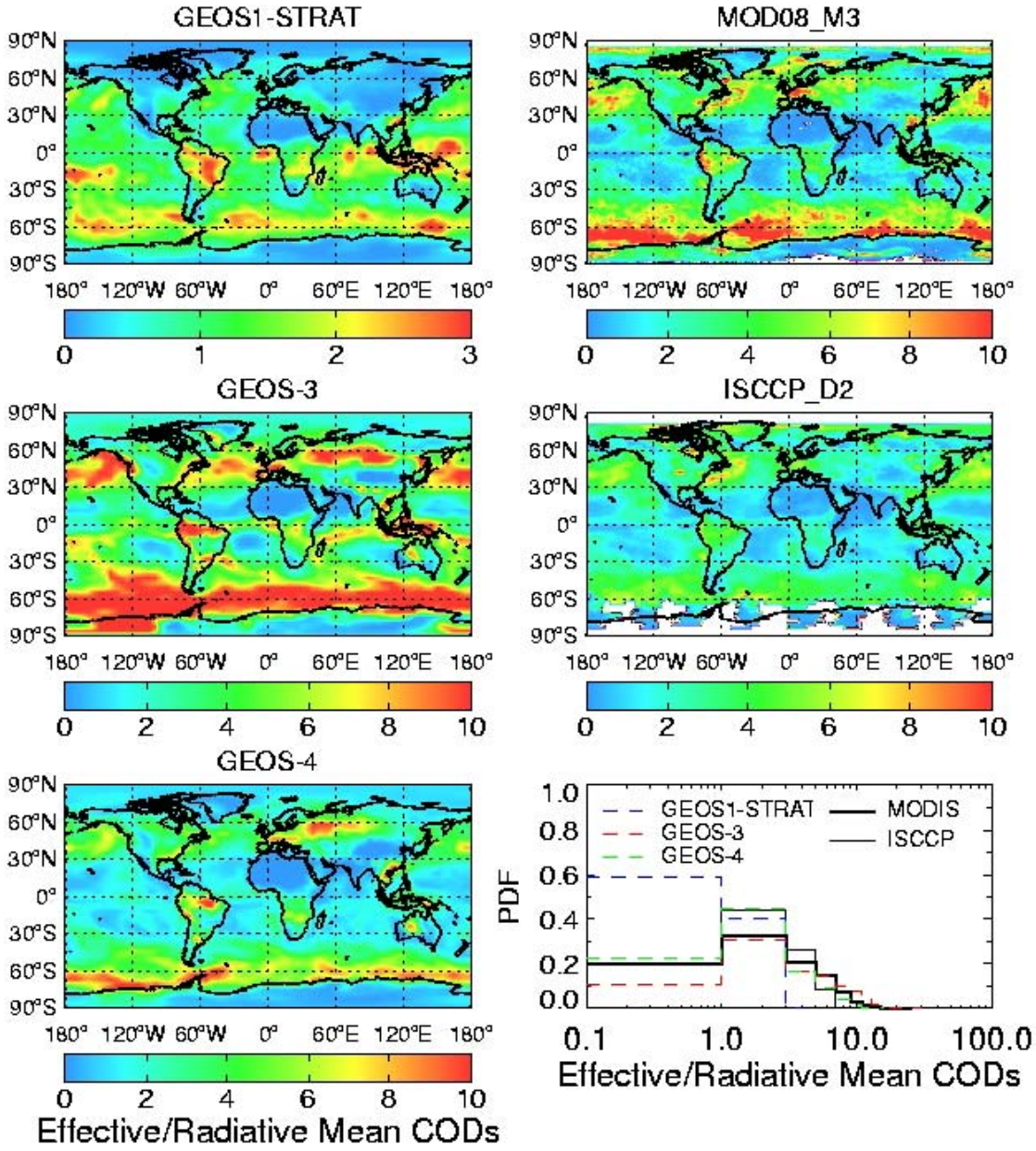

Figure 3. The global distributions of GEOS1-STRAT (1996), GEOS-3 (2001), and GEOS-4 (2001) monthly mean column effective cloud optical depths (left panels) are compared to MODIS and ISCCP retrievals (radiative mean) for March 2001. Note the smaller color scale for GEOS1-STRAT. The Approximate Random Overlap (RAN, see equation 1) is used to calculate GEOS column effective cloud optical depths. MODIS and ISCCP all-sky grid-box mean cloud optical depths are averages over both cloudy and clear regions with nonlinear weights that preserve the average cloud albedo (equation 5). Also shown are the probability distribution functions (PDF) of global monthly mean cloud optical depths in each dataset (right bottom panel). See text for details.

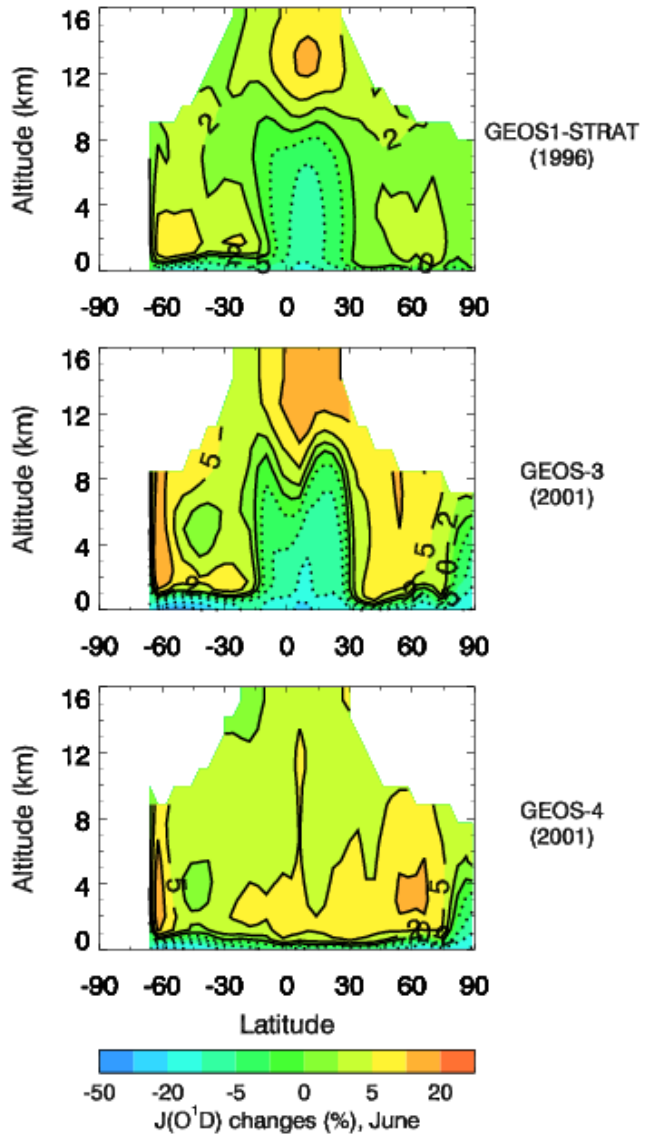

Figure 4. Percentage changes in monthly zonal mean J(O^1D) in the troposphere due to the radiative effects of clouds in June, as simulated by the GEOS-Chem model driven with GEOS1-STRAT (1996), GEOS-3 (2001) and GEOS-4 (2001), respectively. Filled contour levels are -50, -30, -20, -10, -5, -2, 0, 2, 5, 10, 20%. Dotted contours indicate negative changes.

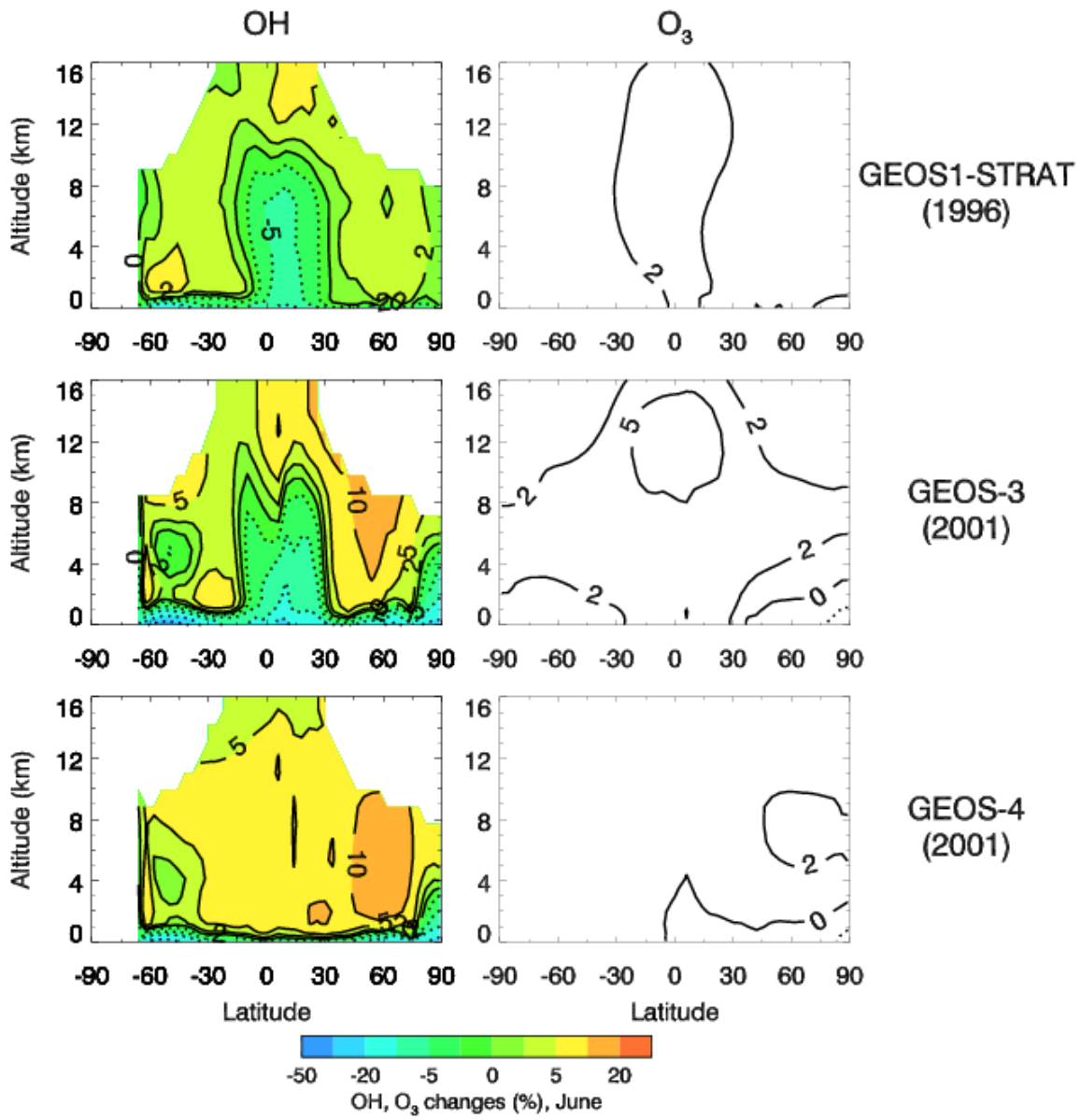

Figure 5. Same as Figure 4, but shown for OH and O_3 concentrations. Contour levels are -50, -30, -20, -10, -5, -2, 0, 2, 5, 10, 20%. Dotted contours indicate negative changes.

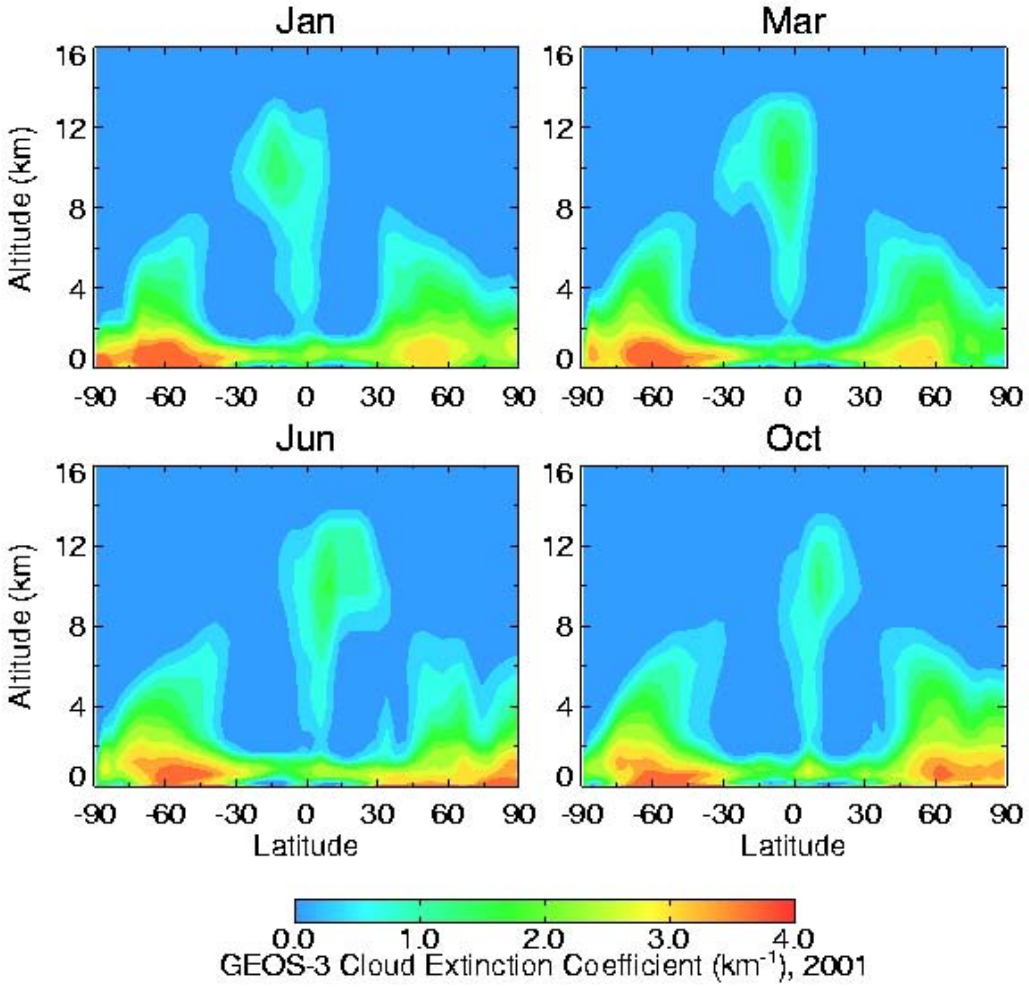

Figure 6. Zonal mean latitude-height cross-sections of GEOS-3 monthly mean cloud extinction coefficient (km^{-1}) for January, March, June and October 2001.

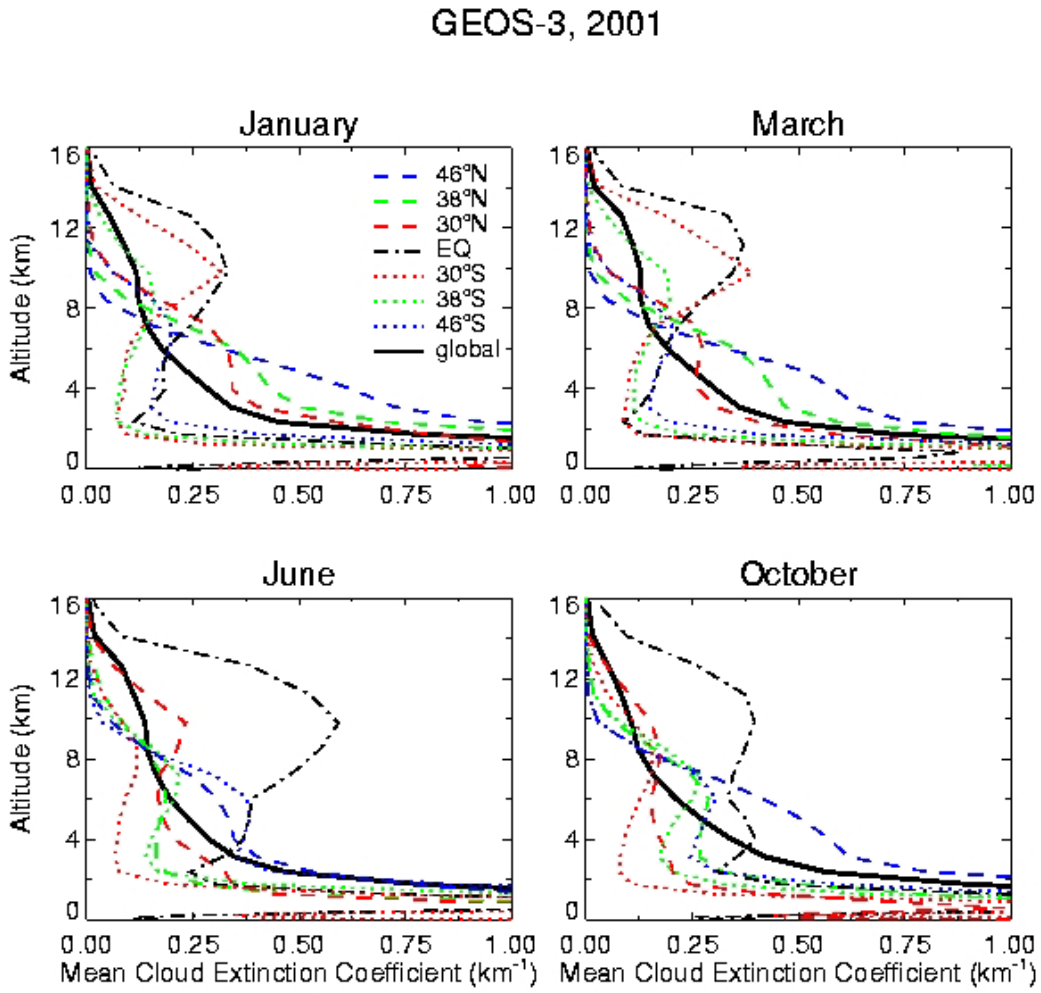

Figure 7. Same as Figure 6, but shown as vertical profiles of monthly zonal mean cloud extinction coefficients (km^{-1}) at selected latitudes (46ºN, 38ºN, 30ºN, equator, 30ºS, 38ºS, and 46ºS) for January, March, June and October 2001. Also shown are averages over all latitudes (solid lines). Vertical profiles between the surface and 3 km where cloud extinction coefficients may exceed 1.0 km^{-1} are shown in Figure 8.

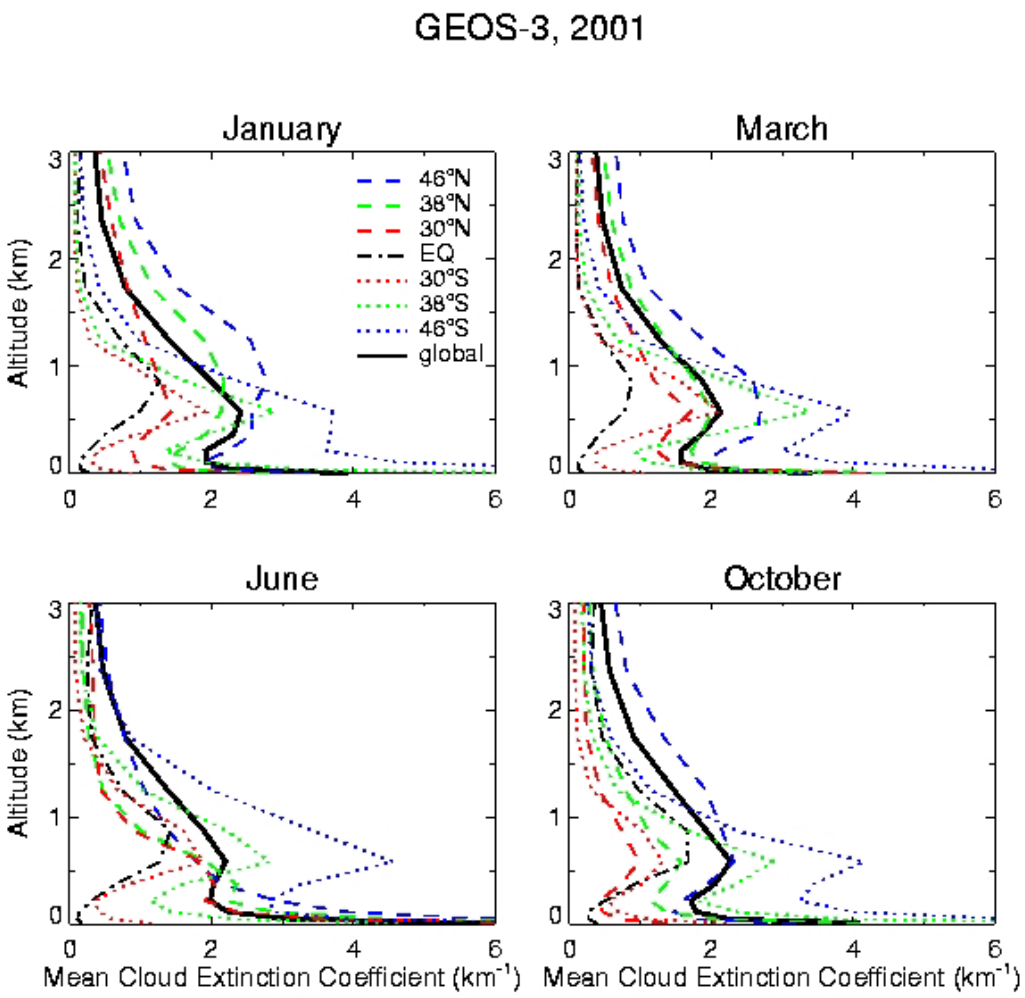

Figure 8. Same as Figure 7, but for the altitudes of 0-3 km.

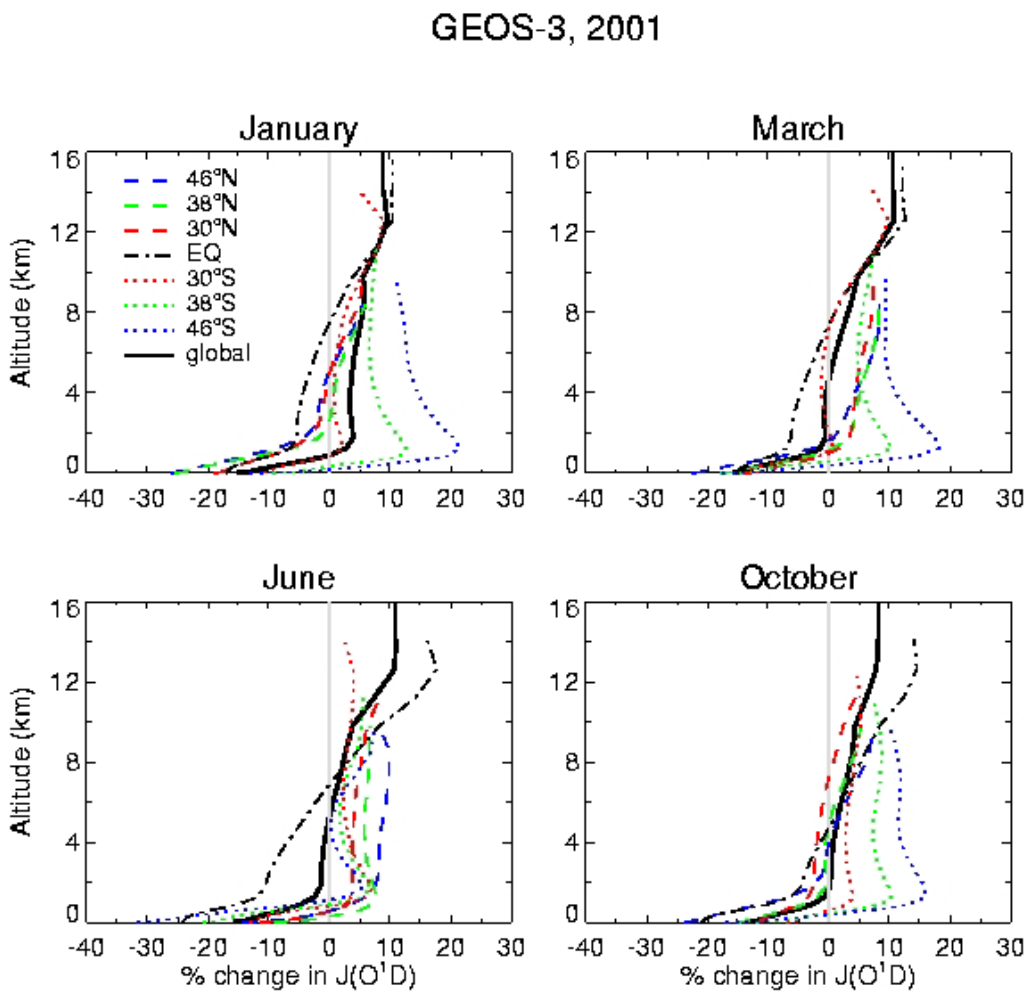

Figure 9. Same as Figure 7, but for percentage changes in monthly zonal mean $J(O^1D)$ due to the radiative effects of clouds.

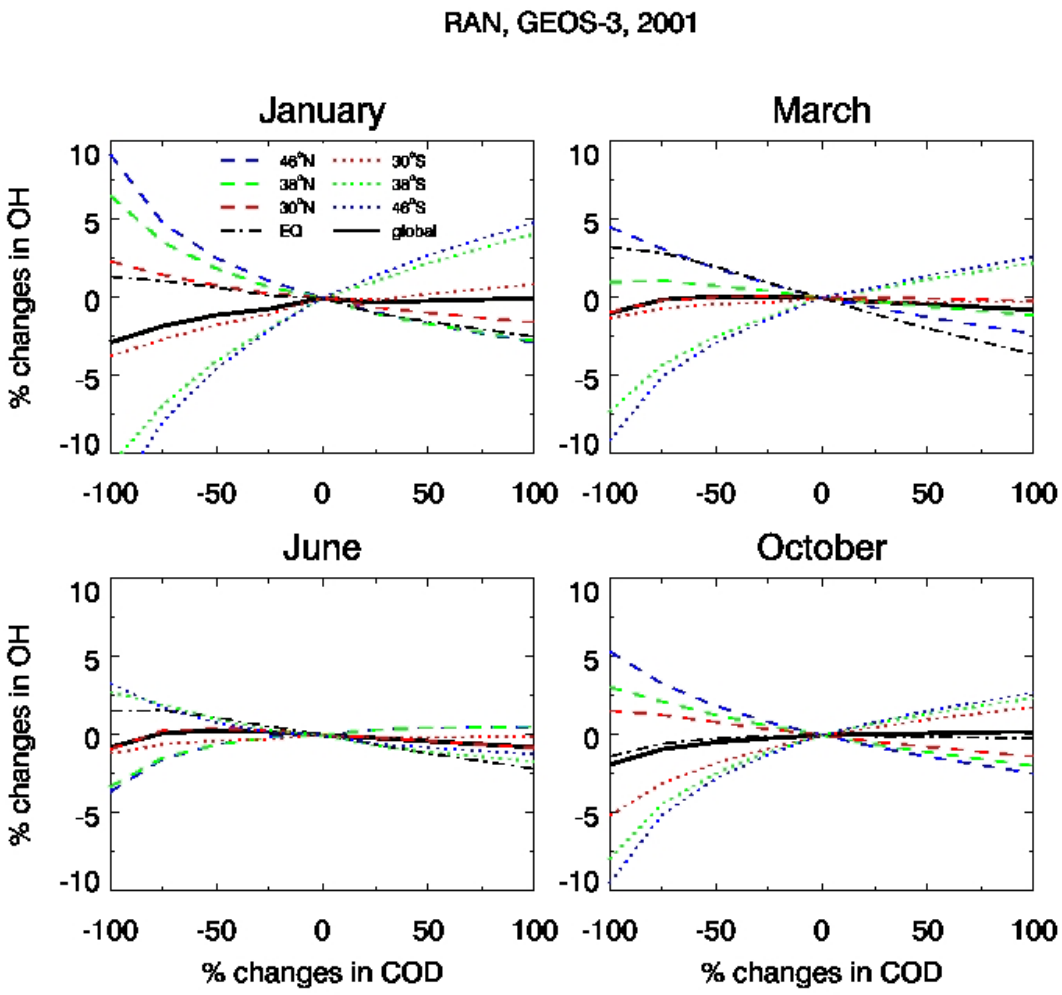

Figure 10. Sensitivities of mean tropospheric OH concentrations to the magnitude of cloud optical depths in January, March, June and October, as simulated by the GEOS-Chem model driven with GEOS-3 (2001). Plotted in the figure are the percentage changes in global (solid lines) and column (at selected latitudes, dot and dashed lines) mean OH relative to the standard simulation as the magnitude of 3-D cloud optical depths is adjusted progressively from -100% to 100%. A -50% change in cloud optical depths corresponds to half of the original GEOS-3 cloud optical depth with the same 3-D spatial distributions.

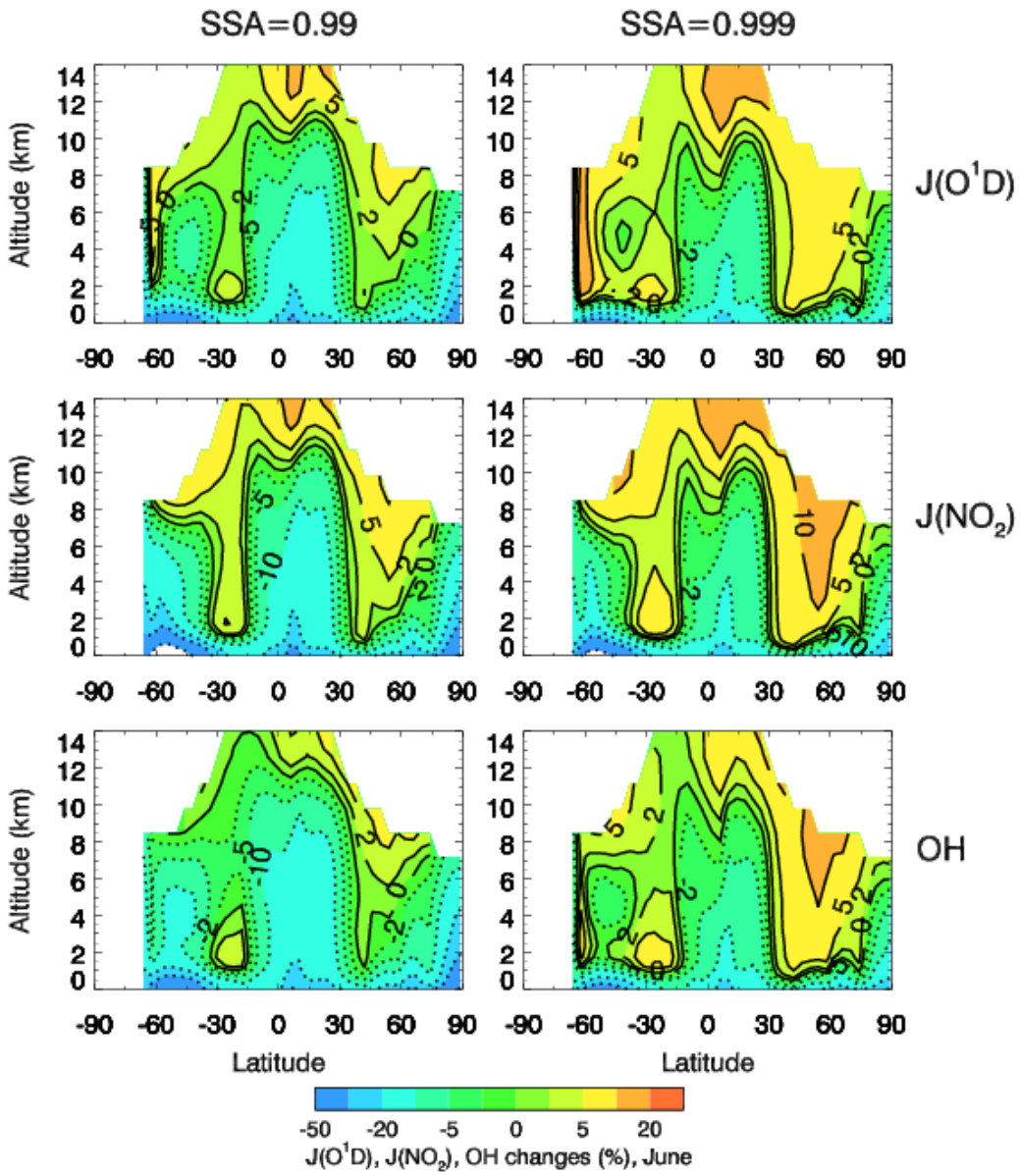

Figure 11. Simulated percentage changes in the June monthly zonal mean $J(O^1D)$, $J(NO_2)$ and OH due to the radiative effects of clouds (GEOS-3, 2001), using cloud SSA=0.99 (left panels) and SSA=0.999 (right panels), respectively.